Title

Neuroanatomical and functional consequences of oxytocin treatment at birth in prairie voles.

Authors

Kenkel, William

Ortiz, Richard

Yee, Jason

et al.

Publication Date

2023-04-01

DOI

10.1016/j.psyneuen.2023.106025

Peer reviewed

HHS Public Access

Author manuscript

Psychoneuroendocrinology. Author manuscript; available in PMC 2024 April 01.

Published in final edited form as:

Psychoneuroendocrinology. 2023 April ; 150: 106025. doi:10.1016/j.psyneuen.2023.106025.

Neuroanatomical and Functional Consequences of Oxytocin Treatment at Birth in Prairie Voles

William M. Kenkel[1,2,*], **Richard J. Ortiz**[2,3,4], **Jason R. Yee**[2,5], **Allison M. Perkeybile**[2,6], **Praveen Kulkarni**[2], **C. Sue Carter**[6], **Bruce S. Cushing**[4], **Craig F. Ferris**[2]

[1]Department of Psychological & Brain Sciences, University of Delaware, Newark, Delaware

[2]Department of Psychology, Center for Translational NeuroImaging, Northeastern University, Boston, Massachusetts

[3]Department of Chemistry and Biochemistry, New Mexico State University, Las Cruces New Mexico

[4]Department of Biological Sciences, University of Texas at El Paso, El Paso, Texas

[5]Institute of Animal Welfare Science, University of Veterinary Medicine, Vienna, Austria

[6]Department of Psychology, University of Virginia, Charlottesville, Virginia

Abstract

Birth is a critical period for the developing brain, a time when surging hormone levels help prepare the fetal brain for the tremendous physiological changes it must accomplish upon entry into the „extrauterine world'. A number of obstetrical conditions warrant manipulations of these hormones at the time of birth, but we know little of their possible consequences on the developing brain. One of the most notable birth signaling hormones is oxytocin, which is administered to roughly 50% of laboring women in the United States prior to / during delivery. Previously, we found evidence for behavioral, epigenetic, and neuroendocrine consequences in adult prairie vole offspring following maternal oxytocin treatment immediately prior to birth. Here, we examined the neurodevelopmental consequences in adult prairie vole offspring following maternal oxytocin treatment prior to birth. Control prairie voles and those exposed to 0.25 mg/kg oxytocin were scanned as adults using anatomical and functional MRI, with neuroanatomy and brain function analyzed as voxel-based morphometry and resting state functional connectivity,

*corresponding author, wm.kenkel@gmail.com.

Disclosures:

All of the authors have contributed substantially to the manuscript. WMK, JRY, and CSC were responsible for concept and experimental design. JRY and AMP carried out the bulk of the experiments. PK and CFF designed much of the neuroimaging technology and analysis pipeline; WMK and JRY adapted it for use in prairie voles. WMK, CFF and RJO were responsible for interpretation. WMK and CFF created the figures. WMK drafted the first version of this manuscript and all authors provided feedback on the finished product.

All data available upon request.

CFF reports a financial interest in Animal Imaging Research, the company that makes the radio frequency electronics and holders for animal imaging. All other authors report no biomedical financial interests or potential conflicts of interest.

respectively. Overall, anatomical differences brought on by oxytocin treatment, while widespread, were generally small, while differences in functional connectivity, particularly among oxytocin-exposed males, were larger. Analyses of functional connectivity based in graph theory revealed that oxytocin-exposed males in particular showed markedly increased connectivity throughout the brain and across several parameters, including closeness and degree. These results are interpreted in the context of the organizational effects of oxytocin exposure in early life and these findings add to a growing literature on how the perinatal brain is sensitive to hormonal manipulations at birth.

Keywords

Oxytocin; Brain; Birth; Development; Prairie vole

1. Introduction:

Oxytocin (OXT) is a potent and pleiotropic hormone that surges at birth to help facilitate the tremendous changes that both mammalian mothers and their offspring must accomplish upon delivery (Kenkel, 2020; Kenkel et al., 2014; Kingsbury and Bilbo, 2019). As of 2019, 29.4% of laboring women in the U.S. received OXT to induce labor (Martin et al., 2021), and according to available survey data, this figure raises to ~50% of birthing women in America when considering OXT used to either induce and/or augment labor (Declercq et al., 2014). This obstetric practice is of interest to neuroscience because there is evidence OXT can cross the placenta (Malek et al., 1996) and a growing literature suggests the neonatal brain is particularly sensitive to OXT around the time of birth, when OXT receptor (*Oxtr*) expression begins to accelerate (Rokicki et al., 2022) and OXT neurons in the brain undergo intense remodeling (Madrigal and Jurado, 2021). Indeed, the long-term, developmental effects of OXT manipulations in early life are well-documented in animal models (Bales and Perkeybile, 2012; Hammock, 2015), which suggests that the perinatal period may be a *sensitive period* with regard to the impact of OXT.

Some initial studies suggested higher rates of autism spectrum and attention deficit / hyperactivity disorder amongst children born to women whose labors were induced with OXT; however, meta-analysis of these findings suggest that any such conclusions remain premature (Lønfeldt et al., 2019) and more recent work examining nationwide registries suggest that such associations likely arose from confounding factors (Lønfeldt et al., 2020; Stokholm et al., 2021). While there have been conflicting reports as to whether OXT administered to induce / augment labor is associated with increased rates of autism spectrum disorder or autistic-like behavior in offspring, considerations of dose add an important degree of nuance to this topic (Guastella et al., 2018; Soltys et al., 2020). Thus, regardless of whether the consequences of obstetrically administered OXT raise to the level of a neurodevelopmental disorder, the question of whether OXT affects offspring neurodevelopment is of great public health relevance given its widespread use.

Previously, we investigated the impact of maternally administered OXT on offspring neurodevelopment and behavior using the socially monogamous prairie vole (Kenkel et al., 2019). We found that fetal physiology was indeed sensitive to maternally administered OXT

and that, in the fetal brain, such OXT dose-dependently increased methylation of the *Oxtr* promoter. In adulthood, OXT-exposed offspring of both sexes were found to demonstrate a broadly gregarious phenotype such that they exhibited more spontaneous alloparental care toward unrelated pups and spent more time in close social contact with opposite-sex adults. Male voles exposed to OXT also showed increased density of OXT receptor in the central amygdala, insular cortex, and parietal cortex, while showing decreased vasopressin receptor 1a density in the ventral pallidum. These findings built upon a substantial body of research, carried out largely in prairie voles, that established long-lasting, often sexually-dimorphic and dose-dependent organizational effects on both brain and behavior following direct treatment of neonatal vole pups with OXT on the first postnatal day (Bales and Carter, 2003; Kramer et al., 2006; Yamamoto et al., 2004).

Because OXT is a pleiotropic hormone, we opted for a broad survey of the brain in the present study, carrying out whole-brain resting functional connectivity to further characterize the scope of the neurodevelopmental consequences of OXT exposure at birth. Here, we used magnetic resonance imaging (MRI) to scan the brains of adult male and female prairie vole offspring originally born to pregnant females treated with 0.25 mg/kg OXT on the expected day of delivery. We examined both anatomical measures (voxel-based morphometry (VBM) and diffusion-weighted imaging (DWI)) as well as functional measures (resting state functional connectivity (rs-fMRI) and several graph theory measures (detailed below).

2. Materials and Methods:

2.1 Subjects

Prairie vole offspring (*Microtus ochrogaster*) were generated as previously described (Kenkel et al., 2019). All procedures were conducted in accordance with the National Institutes of Health Guide for the Care and Use of Laboratory Animals and were approved by the Institutional Animal Care and Use Committee of Northeastern University. On the expected day of delivery, pregnant females were either injected intraperitoneally with OXT (0.25 mg/kg, ‘OXT’) or left undisturbed (‘Control’). Administrations of this dose of OXT to term pregnant females is beneath the threshold to induce precipitous labor. At 0.25 mg/kg, this dose is equivalent to a 5 IU dose in humans, which is within the range of reported doses used clinically (1.8 – 5.5 IU) (Grotegut et al., 2017; Guastella et al., 2018; Soltys et al., 2020).

Offspring were only included if they were delivered within 24 hours of OXT treatment. Offspring were raised by their birth parents as we have previously observed no effect of maternal-OXT treatment on offspring-infant interaction of a similar maternal treatment OXT (Kenkel et al., 2019). At 20 days of age, OXT and Control offspring were weaned into same-sex sibling pairs and were left to mature. Upon reaching adulthood (postnatal days 60–70), OXT and Control offspring underwent three neuroimaging scans: aT1-weighted anatomical scan for voxel based morphometry scan (VBM), an awake, resting state functional scan (rs-fMRI), and an anesthetized diffusion-weighted imaging scan (DWI), as detailed below. Subject offspring consisted of 17 Control females, 19 Control males, 17 OXT-exposed females, and 16 OXT-exposed males. From these, 7 Control females, 12 Control males, 13

OXT-exposed females and 13 OXT-exposed males were ultimately included in the rs-fMRI analyses after removing subjects due to motion artefact or technical difficulties.

2.2 Neuroimaging

All neuroimaging measures were collected using a Bruker BioSpec 7.0T/20-cm Ultra Shield Refrigerated horizontal magnet (Bruker, Billerica, MA). A 20-G/cm magnetic field gradient insert (inner diameter 12 cm) was used to scan anesthetized subjects using a quadrature transmit/receive volume coil (inner diameter 38 mm). Imaging sessions began with an anatomical scan with the following parameters: 20 slices; slice thickness, 0.70 mm; field of view, 2.5 cm; data matrix, 256 x 3 x 256; repetition time, 2.5 seconds; echo time (TE), 12.0 ms; effective TE, 48 ms; number of excitations, 2; and total acquisition time, 80 seconds. VBM yields measures of the volume of each brain region scaled, while DWI yields several measures related to the diffusivity of water within gray matter microarchitecture. The DWI measure apparent diffusion coefficient (ADC) reflects the impedance of water diffusion through Brownian movement in any direction, where high values indicate restricted diffusion. On the other hand, fractional anisotropy (FA) represents the directionality of water diffusion within brain tissue, with low values suggesting less restrictions on water's movement. Finally, rs-fMRI reports the degree of correlation between brain regions in the absence of any stimuli beyond the conditions of scanning.

2.2.1 Voxel Based Morphometry (VBM)—The following procedures were adapted for use in the vole from those described previously for rats (Lawson et al., 2020). For each subject, the atlas (image size 256 x 256 x 63) (H × W × D) was warped from the standard space into the subject image space (image size 256 × 256 × 40) using the nearest-neighbor interpolation method. In the volumetric analysis, each brain region was therefore segmented, and the volume values were extracted for all 111 regions of interest (ROIs), calculated by multiplying unit volume of voxel (in mm^3) by the number of voxels using an in-house MATLAB script. To account for different brain sizes, all ROI volumes were normalized by dividing each subject's ROI volume by their total brain volume.

2.2.2 Diffusion-weighted Imaging (DWI)—The following procedures were identical to those described previously (Ferris et al., 2019; Kulkarni et al., 2020). Diffusion-weighted imaging (DWI) was acquired with a spin-echo echo-planar imaging (EPI) pulse sequence with the following parameters: repetition time/TE, 500/20 ms; 8 EPI segments; and 10 noncollinear gradient directions with a single b-value shell at 1000 seconds/mm^2 and 1 image with a b-value of 0 seconds/mm^2 (referred to as b0). Geometrical parameters were as follows: 48 coronal slices, each 0.313 mm thick (brain volume) and with in-plane resolution of 0.313 x 3 x 0.313 mm^2 (matrix size, 96 x 3 x 96; field of view, 30 mm^2). The imaging protocol was repeated 2 times for signal averaging. DWI acquisition took 35 to 70 minutes. DWI included diffusion-weighted three-dimensional EPI image analysis producing FA maps and apparent diffusion coefficient. DWI analysis was implemented with MATLAB (version 2017b) (The MathWorks, Inc., Natick, MA) and MedINRIA version 1.9.0 (http://www-sop.inria.fr/asclepios/software/MedINRIA/index.php) software.

Each brain volume was registered with the three-dimensional MRI Vole Brain Atlas template (Ekam Solutions LLC, Boston, MA) allowing voxel- and region-based statistics (Yee et al., 2016). In-house MIVA software was used for image transformations and statistical analyses. For each vole, the b0 image was coregistered with the b0 template (using a 6-parameter rigid-body transformation). The coregistration parameters were then applied on the DWI indexed maps for each index of anisotropy. Normalization was performed on the maps providing the most detailed and accurate visualization of brain structures. Normalization parameters were then applied to all indexed maps and then smoothed with a 0.3-mm Gaussian kernel. To ensure that preprocessing did not significantly affect anisotropy values, the nearest neighbor option was used following registration and normalization.

2.2.3 Resting State Functional MRI (rs-fMRI)—We used the same equipment and scanning protocols as in our recent work; for complete details see (Ortiz et al., 2020, 2022; Yee et al., 2016). Data were analyzed as 111 nodes corresponding to brain regions specified in a vole-specific atlas (Yee et al., 2016). Pearson's correlation coefficients were computed per subject across all node pairs (6105), assessing temporal correlations between brain regions. Then, r-values' (−1 to 1) normality were improved using Fisher's Z-transform. For each group, 111×111 symmetric connectivity matrices were constructed, each entry representing the strength of edge. An |Z|=2.3 threshold was used to avoid spurious or weak node connections (Worsley, 2001).

2.2.4 Network Analyses—Graph theory network analysis was generated using Gephi, an open-source network and visualization software (Bastian et al., 2009). For all groups, the absolute values of their respective symmetric connectivity matrices were imported as undirected networks and a threshold of |Z|=2.3 was applied to each node's edges to avoid spurious or weak node connections (Worsley et al., 1992).

2.2.5 Betweenness Centrality—Betweenness centrality analyzes occurrences where a node lies in the path connecting other nodes (Freeman, 1977). Let $n^k_{i,j}$ be the number of pathways from *i* to *j* going through *k*. Using these measures of connection, the betweenness of vertex *k* is:

$$B_k = \sum_{ij} \frac{n^k_{i,j}}{n_{ij}}.$$

2.2.6 Degree Centrality—Degree centrality indicates the number of associations of a specific node (Freeman, 1978). Non-weighted, binary degree is defined as:

$$C_D(j) = \sum_{j=1}^{n} A_{ij}$$

where *n* is the number of rows in the matrix in the adjacency matrix ***A*** and the elements of the matrix are given by A_{ij}, the number of edges between nodes *i* and *j*.

2.2.7 Closeness Centrality—Closeness centrality measures the average distance from a given starting node to all other nodes in the network (Sabidussi, 1966). Closeness is defined as:

$$C(x) = \frac{N-1}{\sum_y d(y,x)}$$

where $d(y,x)$ is the distance between vertices x and y and N is the number of nodes in the graph.

2.3 Statistics

Normality tests of control females, control males, OXT-exposed females and OXT-exposed males were performed to examine if parametric or non-parametric assumptions were required for future analysis. Shapiro-Wilk's tests were performed to examine normality assumption for degree, closeness and betweenness centrality values. Regional p-values that were greater than 0.05 were assumed to be normal. A corresponding list of nodes that classified a region is detailed in table S1. After assumptions of normality were validated, one-way ANOVA tests were used to compare differences in degree, closeness and betweenness centralities between groups. When necessary, a nonparametric Kruskal-Wallis test was performed if there was evidence against normality assumption. Statistical differences between groups were determined using a Mann-Whitney U test (a = 5%). The following formula was used to account for false discovery from multiple comparisons:

$$P(i) \leq \frac{i}{V}\frac{q}{c(V)}$$

P(i) is the p value based on the t test analysis. Each of 111 regions of interest (ROIs) (i) within the brain containing V ROIs. For graph theory measures, statistical analyses were calculated using GraphPad Prism version 9.0.0 for MacOS (GraphPad Software, San Diego, California USA, www.graphpad.com). For post-hoc analyses of graph theory parameters, Holm-Šídák test (for parametric) and Dunn's (for nonparametric) were used after correction for multiple comparisons.

3. Results:

Detailed results can be found in the figures and tables; here, we will address broad patterns such as the number of brain regions affected for a given measure. We observed a number of differences in adult VBM measures after OXT treatment at birth; however, most were small to very small in effect size (Figure 1 and Tables 1–3). Accounting for sex differences was important because we previously found males to be more sensitive in terms to the neuroanatomical effects of OXT treatment at birth (Kenkel et al., 2019). Within the Control group, there was only a single sex difference in regional volume (the reticular nucleus); within the OXT group, however, OXT-exposed males had smaller volumes in 8 of 17 cortical regions and larger volumes in 11 brainstem / cerebellar regions compared to OXT-exposed females (Table 1). Similarly, OXT-exposed males had smaller volumes in 9 of 17 cortical regions and larger volumes in 9 brainstem / cerebellar regions compared to Control males

(Table 2). Comparing within females, OXT treatment at birth resulted in smaller volumes in 4 of 17 cortical regions (Table 3). Control animals generally had larger amygdalar volumes than OXT animals (4 of 6 subregions in males; 2 of 6 in females). When morphometry data from all 111 brain regions were loaded into a PCA, the overall explanatory value of dimensions 1 and 2 was modest (29.4% and 15.9% respectively) and there were impacts of both sex and treatment on dimension 1, with male sex ($F(1,69) = 4.98$, $p = 0.029$) and OXT treatment ($F(1,69) = 16.06$, $p < 0.001$) leading to greater values (Figure 2).

Prairie voles from different populations that show differences in social behaviors regulated by OXT also show differences in functional connectivity and DWI measures of anatomical connectivity (Ortiz et al., 2020, 2022). Here, we observed a broad, albeit subtle pattern of effects in OXT-exposed males in DWI measures. In terms of FA, Control animals showed small but widespread sex differences, with females having greater FA than males across brain regions, a pattern not present in OXT animals due to increased FA among OXT-exposed males (Figure 3A, Tables 2 and 3).In contrast, there were no differences in either FA or ADC between OXT-exposed males and OXT-exposed females, whereas there were 62 and 48 such regions amongst Control animals. When FA data from all 111 brain regions were loaded into a PCA, there were no effects of either sex or treatment detected (Figure 3A). In terms of ADC, Control males had greater ADC values than OXT-exposed males across 84 brain regions (Table 5). While we observed widespread ADC differences between Control males and females, we observed no sex differences in ADC in the OXT-exposed condition. The PCA for ADC revealed a main effect of OXT exposure ($F(1,65) = 5.80$, $p = 0.019$) and a trend toward an interaction between sex and treatment ($p = 0.087$). Post-hoc analysis revealed that Control males had greater dimension 1 values than both OXT-exposed males ($p = 0.026$) and OXT-exposed females ($p = 0.042$). Thus, across the brain, OXT-exposed males' ADC values more closely resembled Control females and OXT-exposed females than they did Control males.

Functional connectivity is influenced by both sex and the OXT system in humans (Hernandez et al., 2020; Satterthwaite et al., 2015; Zhang et al., 2016). In the present analyses of voles' functional connectivity (Figures 4–8), OXT-exposed males stood out as having a widespread pattern of greater connectivity. The vast majority of connections across all groups arose from positive correlations. Male sex and OXT treatment both increased the proportion of significant connections for both positive and negative connections (chi-square $p < 0.001$ for both effects). Whereas Control females were found to have significant functional connectivity in 5% of all possible connections, OXT-exposed females had significant connectivity in 7.2% of connections. Whereas Control males had connectivity in 6.3% of connections, OXT-exposed males had significant connectivity in 12.5% of connections (Figure 4A). Similarly, male sex and OXT treatment at birth both increased the strength of connectivity among region-region pairs whose activity was significantly correlated, but only for positively correlated pairs ($p < 0.001$ for both effects, Figure 4B). Thus, OXT led to more regions significantly functionally connected and stronger correlations in such regions among males and to a lesser extent among females (Figures 4,5). In examining the pattern of results within correlation matrices, we observed a concentration of stronger connectivity among regions of the same cluster (Figure 4D and E). This led us to examine the strength of intra- vs. inter-cluster connectivity as a function of sex and

birth treatment, which revealed that male sex and OXT treatment increased intra-cluster connectivity (e.g. central amygdala and medial amygdala) to a greater degree than inter-cluster connectivity (e.g. central amygdala and dentate gyrus, Figure 4C).

Lastly, we averaged the functional connectivity results within regional clusters to condense and consolidate the large number of findings. As shown in Figure 5, when comparing the strength of connectivity at the level of regional clusters (e.g. all subregions of the amygdala), we observed a treatment effect in the medulla and olfactory system, however there were no significant post-hoc differences. There were also two treatment by sex interactions such that OXT-exposed males had weaker connectivity than OXT-exposed females across the thalamus ($p < 0.002$) and stronger connectivity than OXT-exposed females across the cortex ($p < 0.001$). We then examined three indices from analyses based in graph theory: betweenness, closeness, and degree (see above for definitions of each). In terms of *betweenness,* male sex and OXT treatment both increased betweenness in the basal ganglia (Figure 6, $p < 0.01$ for both effects). In terms of *closeness,* we observed similar albeit more widespread effects, with male sex and OXT treatment and both increasing closeness across several regional clusters (Figure 7). Lastly, similar effects were found in terms of *degree*, with OXT-exposed males having greater degree across a wide swath of regional clusters (Figure 8).

4. Discussion:

Here we describe the effects of injection and exposure to exogenous OXT at birth on neurodevelopment in prairie voles, with consequences seen in neural anatomy and functioning into adulthood. Overall, anatomical differences, while widespread, were generally small, whereas differences in functional connectivity, particularly among OXT-exposed males, were larger. Anatomically, OXT at birth led to a slight reduction in amygdalar volume and OXT-exposed males in particular had slightly smaller cortices and slightly larger brainstem / cerebellums (Tables 1–3). OXT at birth led to males resembling females in terms of FA and ADC (Figure 3). However, functionally, OXT-exposed males showed marked differences from all other groups. OXT at birth led males to display robustly increased functional connectivity throughout the brain (Figures 4–8). This was particularly the case across the cortex in males in terms of the strength, closeness, and degree of connectivity (Figures 5, 7, and 8). Both the number (Figure 4A) and strength (Figure 4B) of positively correlated connections were greater in males and OXT-exposed animals. This was true both within cluster and, to a lesser extent, between clusters as well (Figure 4C). When these effects were examined regionally, few regions stood out (Figure 5); thus, we view these effects as reflecting broad, brain-wide differences. In analyses of brain regions as nodes within a graph, the basal ganglia stood out for both sex and OXT increasing betweenness, whereas such differences were more widespread for closeness and degree. What does this notably broad increase in functional connectivity mean for the OXT-exposed males? We have at present only a few hints.

Interestingly, the observed effects of OXT at birth extended beyond brain regions with dense expression of the OXT receptor. The robust and widespread changes in OXT-exposed males' neural physiology (i.e. functional connectivity) were greater than the changes

observed in neuroanatomy (i.e. VBM and DWI). If OXT-exposed males are continuously experiencing high levels of communication between brain regions, we would expect that to eventually produce changes in anatomical connectedness. Either our anatomical measures of connectivity were insufficiently sensitive to detect these changes, or the relatively small changes in anatomy we did detect are sufficient to produce functional changes that are comparatively more robust. The functional connectivity scans were undertaken with subjects lightly anesthetized, so it is unlikely that OXT-exposed males were responding differentially to the conditions of scanning. Furthermore, we have observed no evidence of stress reactivity being affected by perinatal OXT in our previous studies. OXT acts as a pleiotropic hormone around the time of birth to coordinate the transition from fetal to neonatal life (Kenkel et al., 2014), so by affecting neurodevelopmental trajectory, a single OXT exposure might produce widespread differences across the brain. In mice, seven days of repeated intranasal OXT administration leads to markedly widespread increases in functional connectivity (Pagani et al., 2020). This effect was specific to chronic OXT administration (not seen following acute OXT) and was particularly prominent in connections between cortical regions and the amygdala. When restricting our analysis to only cortico-amygdalar connections, we saw a similar pattern of more and stronger connections in OXT-exposed males (Figure S2). This similarity to our results raises the intriguing possibility that a single OXT administration in early life produces changes similar to chronic OXT administration in adulthood.

We highlight one set of findings in particular because of their relevance to our previous work. As adults, males exposed to OXT via maternal administration at birth had denser OXT receptor distributed along the extent of the agranular insular cortex (Kenkel et al., 2019). In the present study, OXT treatment at birth led to the agranular insular cortex registering as a smaller volume in the brains of adult males (Table 3), along with a slight increase in FA (Table 5) and decrease in ADC (Table 8). Moreover, OXT-exposed males' agranular insular cortex had a greater number of functionally connected regions (35 vs. 19 for Control males) and stronger average connectivity among those regions (z-score 3.45 vs. 2.98 for Control males). Changes in the functioning of the agranular insular cortex correspond to the behavioral effects previously observed, such as increased alloparental caregiving (Kenkel et al., 2019).

In our previous work using the same paradigm of OXT administration to term pregnant prairie voles, we found a dose-dependent increase in the methylation of the OXT receptor promoter within the fetal brain 90 minutes after maternal OXT administration (Kenkel et al., 2019). Importantly, this effect and those discussed above all took place in the context of a cross-fostered experimental design, which ruled out direct effects of OXT on maternal behavior and strongly suggested a direct effect of OXT on the pups. The present findings suggest that there may be long-term consequences of this epigenetic change in OXT receptor regulation at the time of birth, though clearly more work is needed. One intriguing possibility is that by disrupting the inflammatory processes and oxidative stress that normally occur at birth (Kingsbury and Bilbo, 2019), OXT could lead to the rewiring we have seen in this study. Owing to sex differences in susceptibility to oxidative stress at the time of delivery (Minghetti et al., 2013), this could explain the male-biased effects observed here.

Recently, Ortiz et al. employed many of the same measures as those used in the present study in comparing a relatively prosocial population of male prairie voles (deriving from Illinois) with males from a relatively less prosocial population (deriving from an Illinois sire and a less social Kansas dam) (Ortiz et al., 2020, 2022). If we consider the OXT group of the present study as being analogous to the prosocial Illinois voles, we can see similarities in functional connectivity. Both Illinois males and OXT-exposed males showed higher levels of the closeness and degree centrality, particularly within brain regions associated with prosocial behavior. When restricting our analysis to only the prosocial core (Ortiz et al., 2022), we observed a main effect of birth treatment such that OXT led to stronger connectivity, similar to the Illinois males (Figure S3). However, this study's OXT-exposed males did not resemble the prosocial Illinois males anatomically, as the latter displayed higher ADC values in regions associated with prosocial behavior.

Although OXT has been proposed as a treatment in autism spectrum disorders (Alvares et al., 2017), OXT has also been implicated in the etiology of autism spectrum disorders. For example, while some epidemiological studies have suggested a link between autism spectrum disorders and perinatal OXT exposure (Lønfeldt et al., 2019), residual confounding by either genetic or environmental vulnerabilities, could explain this apparent association. One pattern generally observed in the brains of humans with autism spectrum disorders is diminished long-distance functional connectivity and increased short-distance functional connectivity (O'Reilly et al., 2017; Rane et al., 2015). We observed that both male sex and OXT treatment at birth led to increased intra-cluster connectivity (analogous to increased short-distance hyperconnectivity), but also to increased inter-cluster connectivity, though to a lesser extent. Thus, the present results do not entirely resemble the equivalent effects seen in humans with autism spectrum disorders. In our previous work, we observed a broadly gregarious phenotype in OXT-exposed voles (Kenkel et al., 2019); if such results translated to humans, they would support the contention that underlying vulnerabilities bring on both a need for OXT in the mother and susceptibility to autism spectrum disorders in the child. While our previous work found behavioral differences in both males and females exposed to OXT, which is somewhat in contrast to the present study's findings, we also found males to be much more affected by perinatal OXT in terms of neuroanatomy, which was assessed as the density of OXT and AVP receptors -and that finding matches those of the present study. Numerous previous studies have found sex-, dose-, and region-dependent effects of early life OXT manipulation (Carter, 2003; Hammock, 2015).

In the present study, we observed greater intra-cluster as well as inter-cluster connectivity in male voles. In human neuroimaging, a consensus appeared to be forming such that males show greater inter-cluster connectivity whereas females show greater intra-cluster connectivity (Allen et al., 2011; Satterthwaite et al., 2015; Tomasi and Volkow, 2012). However, more recent work has challenged this, finding greater local clustering in males (Zhang et al., 2016). Among neurotypical individuals of both sexes, increased genetic risk load for autism spectrum disorders within the OXT receptor gene is associated with greater functional connectivity between the nucleus accumbens and prefrontal cortex (Hernandez et al., 2020). We observed very little functional connectivity between the prefrontal cortex and any region of the basal ganglia in any of the four groups of the present study. Thus, a floor

effect may have prevented the detection of any OXT-induced consequences for prefrontal cortex / basal ganglia connectivity.

There have been very few studies on the impact of birth interventions and subsequent brain development (Kenkel, 2020; Kenkel et al., 2014). In the realm of neuroanatomy, Chiesa et al. (2021) recently reported that cesarean section results in smaller brain volumes in neonatal mouse pups (Chiesa et al., 2021). However, no such findings have been reported in human children or infants (Deoni et al., 2019). In terms of VBM and functional connectivity in the present study, OXT-exposed males showed a more masculinized phenotype. However, in terms of ADC and FA, OXT led males demonstrated a more feminized phenotype. Further work is needed to reveal the meanings of these differences.

Limitations:

In this study the un-treated “Control” group did not receive a vehicle treatment or other manipulations. Whether the stress of injection given to the mother has a significant consequence for these measures cannot be determined from the current study. However, in a small validation study, adult offspring of saline-treated dams (n = 3 female, 5 male adult offspring) were not found to have meaningful differences in DWI values compared to the un-treated Control animals of the present study (n = 17 female, 19 male adult offspring). It would be difficult to disentangle maternal stress from OXT exposure in humans, as labor augmentation with OXT is associated with a more negative subjective birth experience and increased rates of spinal epidural usage indicating increased need for pain management (Joensuu et al., 2022). That said, a more translationally relevant approach here would have been to maintain steady level of OXT infusion over a long period of time, as takes place in the clinical setting. Such an approach has recently been employed in rats using microinfusion pumps (Giri et al., 2022). Pharmacodynamic considerations are important because OXT administration leads to the internalization and downregulation of the OXT receptor. For instance, stimulating OXT receptors with administration of an OXT agonist leads to 50–60% of receptors internalized (Gimpl and Fahrenholz, 2001; Smith et al., 2006). In our previous study on the methylation of the OXT receptor promoter, we found no difference between saline-injected and non-injected pups (Kenkel et al., 2019).

The data from this study suggest that OXT experienced by a fetus during the perinatal period could have lasting neural consequences. The results also point to the importance of comparing males and females with brain-region specific analyses. Collectively, these findings support the hypothesis that the perinatal brain is sensitive to OXT administered indirectly to the pregnant female. However, it is not possible to determine whether the specific effects measured here are direct or perhaps indirect effects of exogenous OXT, for example via uterine contractions or maternal distress. Finally, in this study, we have also applied several metrics to our fMRI data that have not previously used in prairie voles.

5. Conclusion

As the first experiment of its kind, the outcome of the present study must be considered preliminary, but also suggestive of the need for future investigation of the possible development consequences of perinatal peptides, including those administered to the mother.

We suggest that given the widespread use in obstetric care of OXT for labor induction / augmentation, currently found in the majority of births in the U.S. (Declercq et al., 2014; Martin et al., 2021), a more complete understanding of the neurodevelopmental effects of OXT exposure at delivery is imperative. It is also important to note that the vast majority of deliveries now use OXT during the third stage of labor to prevent postpartum hemorrhage (Miranda et al., 2013; Salati et al., 2019). Delayed cord clamping is becoming standard practice ("Committee Opinion No. 684 Summary," 2017), and this procedure may extend both the duration and dose of potential OXT exposure by the neonate. Because the perinatal period is a sensitive period for brain development in general and possibly in terms of OXT exposure, these practices deserve further investigation. Our findings suggest that prairie voles could help to inform these clinical practices by offering an experimental platform for the examination of long-term consequences of manipulations such as these.

Supplementary Material

Refer to Web version on PubMed Central for supplementary material.

Acknowledgements

This work was supported by the Larry P. Jones Distinguished Professorship Endowment through the University of Texas El Paso (to BSC), a grant from the Eunice Kennedy Shriver National Institute of Child Health and Development (NICHD), P01HD075750 (to CSC and CFF), and the National Institute of General Medical Sciences (5R25GM069621-17 (to RJO)). We would also like to acknowledge the contributions of Kelsey Moore, Jessica Amacker, Emily Grimsley, Megan Barnes, Naomi Zingman-Daniels, Danielle Whalen, Brenda Yeung, Alexander Ian Moore, and Tedi Rosenstein.

REFERENCES:

Allen E, Erhardt E, Damaraju E, Gruner W, Segall J, Silva R, Havlicek M, Rachakonda S, Fries J, Kalyanam R, Michael A, Caprihan A, Turner J, Eichele T, Adelsheim S, Bryan A, Bustillo J, Clark V, Feldstein Ewing S, Filbey F, Ford C, Hutchison K, Jung R, Kiehl K, Kodituwakku P, Komesu Y, Mayer A, Pearlson G, Phillips J, Sadek J, Stevens M, Teuscher U, Thoma R, Calhoun V, 2011. A Baseline for the Multivariate Comparison of Resting-State Networks. Frontiers in Systems Neuroscience 5

Alvares GA, Quintana DS, Whitehouse AJO, 2017. Beyond the hype and hope: Critical considerations for intranasal oxytocin research in autism spectrum disorder. Autism Research 10, 25–41. 10.1002/aur.1692 [PubMed: 27651096]

Bales KL, Carter CS, 2003. Developmental exposure to oxytocin facilitates partner preferences in male prairie voles (Microtus ochrogaster). Behav.Neurosci 117, 854–859. [PubMed: 12931969]

Bales KL, Perkeybile AM, 2012. Developmental experiences and the oxytocin receptor system. Horm.Behav 61, 313–319. 10.1016/j.yhbeh.2011.12.013 [PubMed: 22245313]

Bastian M, Heymann S, Jacomy M, 2009. Gephi: An Open Source Software for Exploring and Manipulating Networks Proceedings of the International AAAI Conference on Web and Social Media 3, 361–362.

Carter CS, 2003. Developmental consequences of oxytocin. Physiol Behav 79, 383–97. [PubMed: 12954433]

Chiesa M, Rabiei H, Riffault B, Ferrari DC, Ben-Ari Y, 2021. Brain Volumes in Mice are Smaller at Birth After Term or Preterm Cesarean Section Delivery. Cereb Cortex 10.1093/cercor/bhab033

Committee Opinion No. 684 Summary: Delayed Umbilical Cord Clamping After Birth, 2017. . Obstetrics & Gynecology 129, 232–233. 10.1097/AOG.0000000000001855

Declercq ER, Sakala C, Corry MP, Applebaum S, Herrlich A, 2014. Major Survey Findings of Listening to MothersSM III: Pregnancy and Birth. J Perinat Educ 23, 9–16. 10.1891/1058-1243.23.1.9 [PubMed: 24453463]

Deoni SC, Adams SH, Li X, Badger TM, Pivik RT, Glasier CM, Ramakrishnaiah RH, Rowell AC, Ou X, 2019. PMC6330134; Cesarean Delivery Impacts Infant Brain Development. AJNR Am.J.Neuroradiol 40, 169–177. 10.3174/ajnr.A5887 [PubMed: 30467219]

Ferris CF, Nodine S, Pottala T, Cai X, Knox TM, Fofana FH, Kim S, Kulkarni P, Crystal JD, Hohmann AG, 2019. Alterations in brain neurocircuitry following treatment with the chemotherapeutic agent paclitaxel in rats. Neurobiology of Pain 6, 100034. 10.1016/j.ynpai.2019.100034 [PubMed: 31223138]

Freeman LC, 1978. Centrality in social networks conceptual clarification. Social Networks 1, 215–239. 10.1016/0378-8733(78)90021-7

Freeman LC, 1977. A Set of Measures of Centrality Based on Betweenness. Sociometry 40, 35–41. 10.2307/3033543

Gimpl G, Fahrenholz F, 2001. The oxytocin receptor system: structure, function, and regulation. Physiol Rev 81, 629–83. [PubMed: 11274341]

Giri T, Jiang J, Xu Z, McCarthy R, Halabi CM, Tycksen E, Cahill AG, England SK, Palanisamy A, 2022. Labor induction with oxytocin in pregnant rats is not associated with oxidative stress in the fetal brain. Sci Rep 12, 3143. 10.1038/s41598-022-07236-x [PubMed: 35210555]

Grotegut CA, Lewis LL, Manuck TA, Allen TK, James AH, Seco A, Deneux-Tharaux C, 2017. The Oxytocin Product Correlates with Total Oxytocin Received during Labor: A Research Methods Study. Am.J.Perinatol 2017/08/15. 10.1055/s-0037-1606119

Guastella AJ, Cooper MN, White CRH, White MK, Pennell CE, Whitehouse AJO, 2018. Does perinatal exposure to exogenous oxytocin influence child behavioural problems and autistic-like behaviours to 20 years of age? J.Child Psychol.Psychiatry 2018/04/28 10.1111/jcpp.12924

Hammock EAD, 2015. Developmental Perspectives on Oxytocin and Vasopressin. Neuropsychopharmacology 40, 24–42. 10.1038/npp.2014.120 [PubMed: 24863032]

Hernandez LM, Lawrence KE, Padgaonkar NT, Inada M, Hoekstra JN, Lowe JK, Eilbott J, Jack A, Aylward E, Gaab N, Van Horn JD, Bernier RA, McPartland JC, Webb SJ, Pelphrey KA, Green SA, Geschwind DH, Bookheimer SY, Dapretto M, On behalf of the, G.C., 2020. Imaging-genetics of sex differences in ASD: distinct effects of OXTR variants on brain connectivity. Translational Psychiatry 10, 82. 10.1038/s41398-020-0750-9 [PubMed: 32127526]

Joensuu J, Saarijärvi H, Rouhe H, Gissler M, Ulander V-M, Heinonen S, Torkki P, Mikkola T, 2022. Maternal childbirth experience and pain relief methods: a retrospective 7-year cohort study of 85 488 parturients in Finland. BMJ Open 12, e061186. 10.1136/bmjopen-2022-061186

Kenkel W, 2020. Birth signalling hormones and the developmental consequences of caesarean delivery. Journal of Neuroendocrinology n/a, e12912. 10.1111/jne.12912

Kenkel WM, Perkeybile AM, Yee JR, Pournajafi-Nazarloo H, Lillard TS, Ferguson EF, Wroblewski KL, Ferris CF, Carter CS, Connelly JJ, 2019. Behavioral and epigenetic consequences of oxytocin treatment at birth. Science Advances 5, eaav2244. 10.1126/sciadv.aav2244 [PubMed: 31049395]

Kenkel WM, Yee JR, Carter CS, 2014. Is oxytocin a maternal-foetal signalling molecule at birth? Implications for development. Journal of neuroendocrinology 26, 739–49. 10.1111/jne.12186 [PubMed: 25059673]

Kingsbury MA, Bilbo SD, 2019. The inflammatory event of birth: How oxytocin signaling may guide the development of the brain and gastrointestinal system. Front.Neuroendocrinol 55, 100794. 10.1016/j.yfrne.2019.100794 [PubMed: 31560883]

Kramer KM, Choe C, Carter CS, Cushing BS, 2006. Developmental effects of oxytocin on neural activation and neuropeptide release in response to social stimuli. Hormones and behavior 49, 206–14. 10.1016/j.yhbeh.2005.07.001 [PubMed: 16112115]

Kulkarni P, Grant S, Morrison TR, Cai X, Iriah S, Kristal BS, Honeycutt J, Brenhouse H, Hartner JC, Madularu D, Ferris CF, 2020. Characterizing the human APOE epsilon 4 knock-in transgene in female and male rats with multimodal magnetic resonance imaging. Brain Research 1747, 147030. 10.1016/j.brainres.2020.147030 [PubMed: 32745658]

Lawson CM, Rentrup KFG, Cai X, Kulkarni PP, Ferris CF, 2020. Using multimodal MRI to investigate alterations in brain structure and function in the BBZDR/Wor rat model of type 2 diabetes. Animal Models and Experimental Medicine 3, 285–294. 10.1002/ame2.12140 [PubMed: 33532703]

Lønfeldt NN, Strandberg-Larsen K, Verhulst FC, Plessen KJ, Lebowitz ER, 2020. Birth with Synthetic Oxytocin and Risk of Childhood Emotional Disorders: A Danish Population-based Study. Journal of Affective Disorders 274, 112–117. 10.1016/j.jad.2020.04.067 [PubMed: 32469793]

Lønfeldt NN, Verhulst FC, Strandberg-Larsen K, Plessen KJ, Lebowitz ER, 2019. Assessing risk of neurodevelopmental disorders after birth with oxytocin: a systematic review and meta-analysis. Psychological Medicine 49, 881–890. 10.1017/S0033291718003021 [PubMed: 30444210]

Madrigal MP, Jurado S, 2021. Specification of oxytocinergic and vasopressinergic circuits in the developing mouse brain. Commun Biol 4, 1–16. 10.1038/s42003-021-02110-4 [PubMed: 33398033]

Malek A, Blann E, Mattison DR, 1996. Human placental transport of oxytocin. J.Matern.Fetal 5, 245–255. 10.1002/(SICI)1520-6661(199609/10)5:5<245::AID-MFM3>3.0.CO;2-H

Martin JA, Hamilton BE, Osterman MJK, Driscoll AK, 2021. Births: Final Data for 2019. Natl Vital Stat Rep 70, 1–51.

Minghetti L, Greco A, Zanardo V, Suppiej A, 2013. Early-life sex-dependent vulnerability to oxidative stress: the natural twining model. The Journal of Maternal-Fetal & Neonatal Medicine 26, 259–262. 10.3109/14767058.2012.733751 [PubMed: 23020682]

Miranda JE, Rojas-Suarez J, Paternina A, Mendoza R, Bello C, Tolosa JE, 2013. The effect of guideline variations on the implementation of active management of the third stage of labor. Int.J.Gynaecol.Obstet. 2013/03/27 10.1016/j.ijgo.2012.12.016

O'Reilly C, Lewis JD, Elsabbagh M, 2017. Is functional brain connectivity atypical in autism? A systematic review of EEG and MEG studies. PLoS ONE 12.

Ortiz R, Yee JR, Kulkarni PP, Solomon NG, Keane B, Cai X, Ferris CF, Cushing BS, 2020. Differences in Diffusion-Weighted Imaging and Resting-State Functional Connectivity Between Two Culturally Distinct Populations of Prairie Vole. Biological Psychiatry: Cognitive Neuroscience and Neuroimaging 10.1016/j.bpsc.2020.08.014

Ortiz RJ, Wagler AE, Yee JR, Kulkarni PP, Cai X, Ferris CF, Cushing BS, 2022. Functional Connectivity Differences Between Two Culturally Distinct Prairie Vole Populations: Insights Into the Prosocial Network. Biological Psychiatry: Cognitive Neuroscience and Neuroimaging 7, 576–587. 10.1016/j.bpsc.2021.11.007 [PubMed: 34839018]

Pagani M, De Felice A, Montani C, Galbusera A, Papaleo F, Gozzi A, 2020. Acute and Repeated Intranasal Oxytocin Differentially Modulate Brain-wide Functional Connectivity. Neuroscience, Animal Models of Neurodevelopmental Disorders 445, 83–94. 10.1016/j.neuroscience.2019.12.036

Rane P, Cochran D, Hodge SM, Haselgrove C, Kennedy DN, Frazier JA, 2015. Connectivity in Autism: A Review of MRI Connectivity Studies. Harv.Rev.Psychiatry 23, 223–244. 10.1097/hrp.0000000000000072 [PubMed: 26146755]

Rokicki J, Kaufmann T, de Lange A-MG, van der Meer D, Bahrami S, Sartorius AM, Haukvik UK, Steen NE, Schwarz E, Stein DJ, Nærland T, Andreassen OA, Westlye LT, Quintana DS, 2022. Oxytocin receptor expression patterns in the human brain across development. Neuropsychopharmacol. 47, 1550–1560. 10.1038/s41386-022-01305-5

Sabidussi G, 1966. The centrality index of a graph. Psychometrika 31, 581–603. 10.1007/BF02289527 [PubMed: 5232444]

Salati JA, Leathersich SJ, Williams MJ, Cuthbert A, Tolosa JE, 2019. Prophylactic oxytocin for the third stage of labour to prevent postpartum haemorrhage. Cochrane Database of Systematic Reviews 10.1002/14651858.CD001808.pub3

Satterthwaite TD, Wolf DH, Roalf DR, Ruparel K, Erus G, Vandekar S, Gennatas ED, Elliott MA, Smith A, Hakonarson H, Verma R, Davatzikos C, Gur RE, Gur RC, 2015. Linked Sex Differences in Cognition and Functional Connectivity in Youth. Cerebral Cortex 25, 2383–2394. 10.1093/cercor/bhu036 [PubMed: 24646613]

Smith MP, Ayad VJ, Mundell SJ, McArdle CA, Kelly E, López Bernal A, 2006. Internalization and Desensitization of the Oxytocin Receptor Is Inhibited by Dynamin and Clathrin Mutants in Human

Embryonic Kidney 293 Cells. Molecular Endocrinology 20, 379–388. 10.1210/me.2005-0031 [PubMed: 16179383]

Soltys SM, Scherbel JR, Kurian JR, Diebold T, Wilson T, Hedden L, Groesch K, Diaz-Sylvester PL, Botchway A, Campbell P, Loret de Mola JR, 2020. An association of intrapartum synthetic oxytocin dosing and the odds of developing autism. Autism 24, 1400–1410. 10.1177/1362361320902903 [PubMed: 32054311]

Stokholm L, Juhl M, Talge NM, Gissler M, Obel C, Strandberg-Larsen K, 2021. Obstetric oxytocin exposure and ADHD and ASD among Danish and Finnish children. International Journal of Epidemiology 50, 446–456. 10.1093/ije/dyaa076 [PubMed: 32535618]

Tomasi D, Volkow ND, 2012. Gender differences in brain functional connectivity density. Human Brain Mapping 33, 849–860. 10.1002/hbm.21252 [PubMed: 21425398]

Worsley KJ, 2001. Statistical analysis of activation images, in: Functional Magnetic Resonance Imaging Oxford University Press, Oxford. 10.1093/acprof:oso/9780192630711.003.0014

Worsley KJ, Evans AC, Marrett S, Neelin P, 1992. A Three-Dimensional Statistical Analysis for CBF Activation Studies in Human Brain. J Cereb Blood Flow Metab 12, 900–918. 10.1038/jcbfm.1992.127 [PubMed: 1400644]

Yamamoto Y, Cushing BS, Kramer KM, Epperson PD, Hoffman GE, Carter CS, 2004. Neonatal manipulations of oxytocin alter expression of oxytocin and vasopressin immunoreactive cells in the paraventricular nucleus of the hypothalamus in a gender-specific manner. Neuroscience 125, 947–55. 10.1016/j.neuroscience.2004.02.028 [PubMed: 15120854]

Yee JR, Kenkel WM, Kulkarni P, Moore K, Perkeybile AM, Toddes S, Amacker JA, Carter CS, Ferris CF, 2016. BOLD fMRI in awake prairie voles: A platform for translational social and affective neuroscience. Neuroimage 138, 221–232. 10.1016/j.neuroimage.2016.05.046 [PubMed: 27238726]

Zhang C, Cahill ND, Arbabshirani MR, White T, Baum SA, Michael AM, 2016. Sex and Age Effects of Functional Connectivity in Early Adulthood. Brain Connectivity 6, 700–713. 10.1089/brain.2016.0429 [PubMed: 27527561]

Highlights

- Voles exposed to oxytocin at birth had functional and anatomical brain changes.
- Male voles were particularly sensitive to oxytocin exposure at birth.
- Oxytocin males had increased functional connectivity throughout the brain.

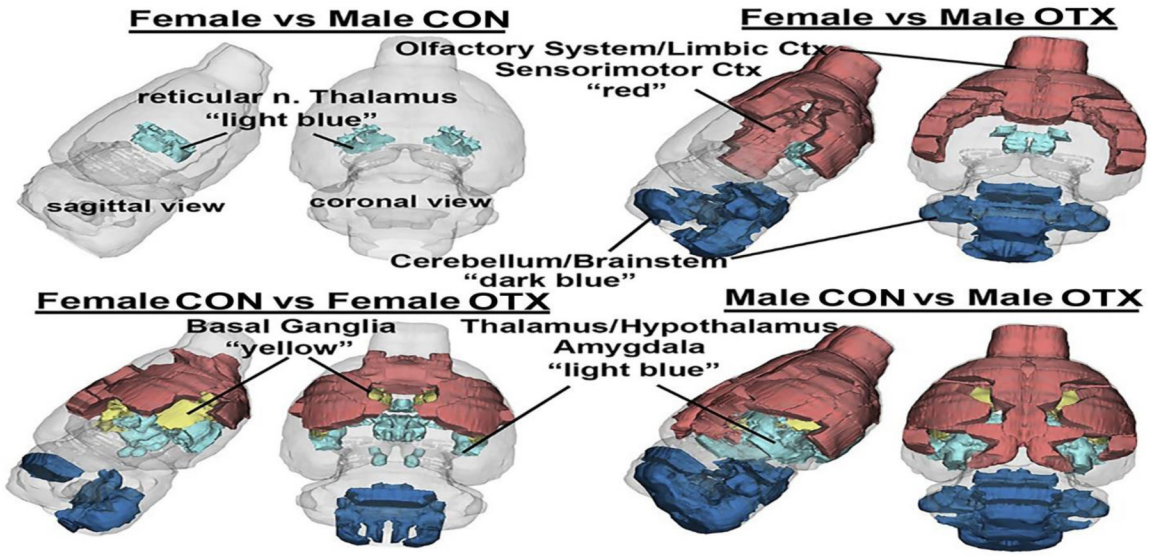

Figure 1.

A 3D color coded reconstructions summarizing the significantly different brain areas with volumetric changes for each experimental condition. Details of these differences can be found in tables 1–3.

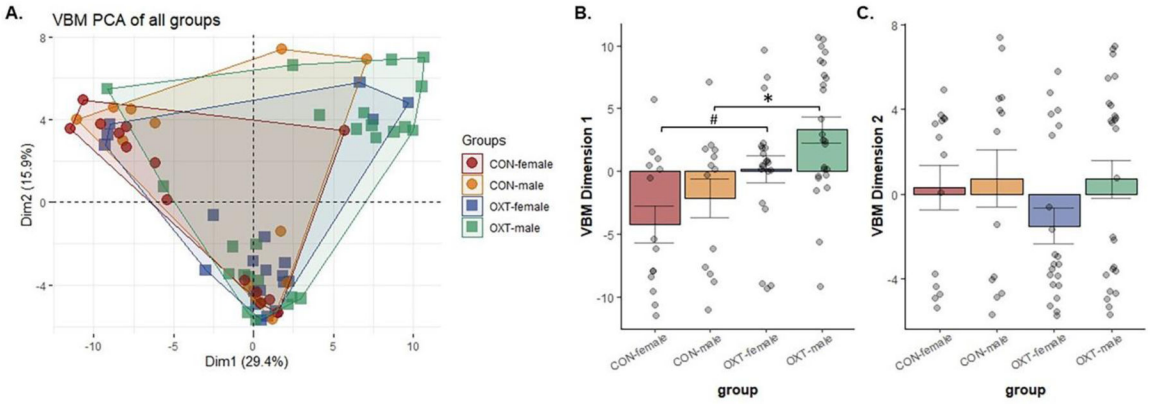

Figure 2.

(A) Voxel-based morphometry (VBM) measures from 111 brain regions were loaded into a principal component analysis. The overall explanatory value of dimensions 1 and 2 was 29.4% and 15.9%, respectively. (B) Both male sex and OXT treatment lead to greater values in dimension 1 ($p < 0.029$ for both comparisons). Post-hoc analyses revealed OXT-exposed males had significantly greater dimension 1 scores than Control males (* $p = 0.017$), while OXT-exposed females tended to be greater than Control females (# $p = 0.079$). (C) There were no effects in dimension 2.

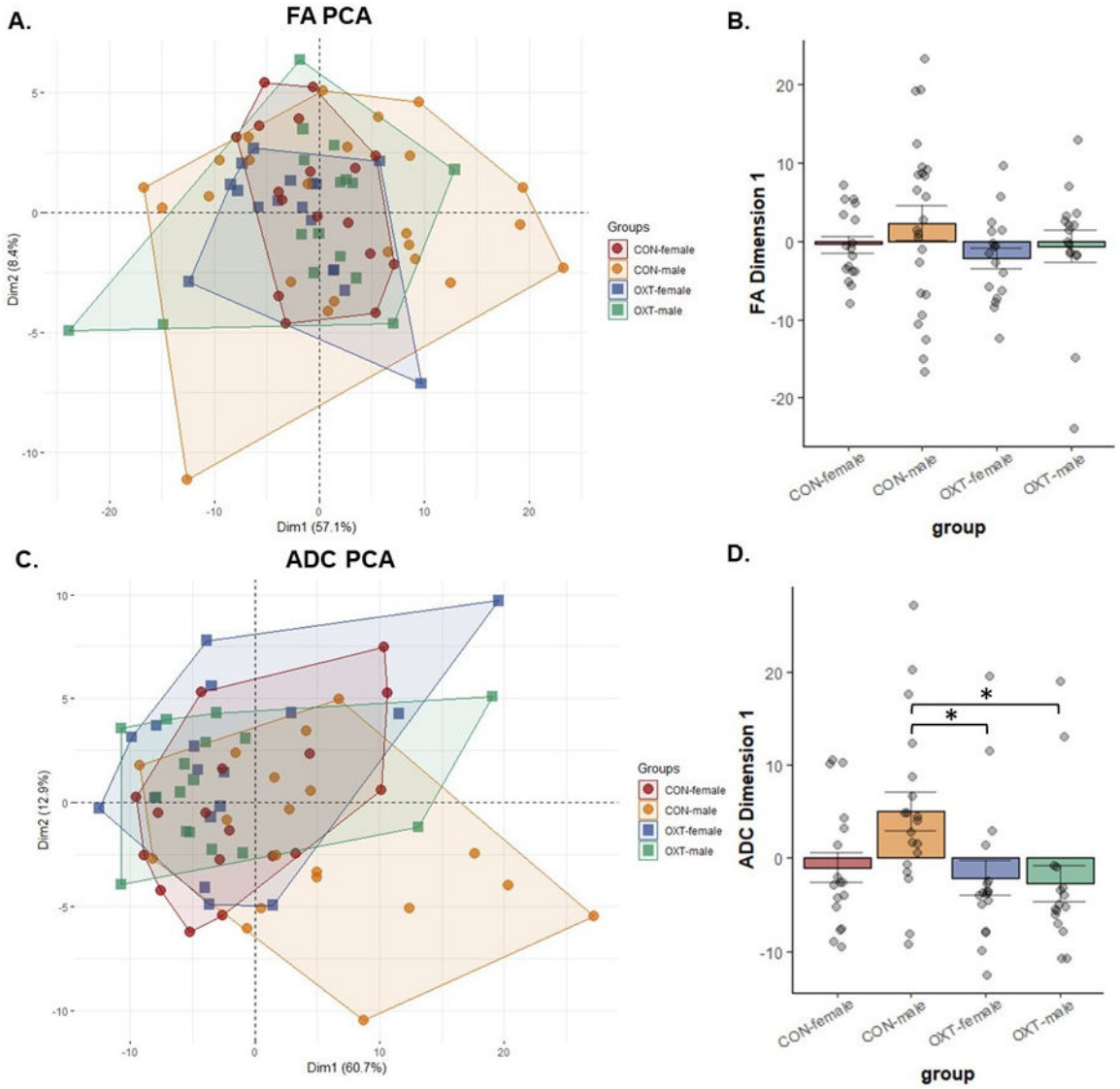

Figure 3.

Diffusion-weighted imaging (DWI) measures for fractional anisotropy (FA, panels A and B) and apparent diffusion coefficient (ADC, panels C and D) from 111 brain regions were loaded into a principal component analysis. (B) There were no significant differences in FA. (D) Control males had greater dimension 1 scores than OXT-exposed males (* $p = 0.026$) and OXT-exposed females (* $p = 0.042$). in terms of ADC.

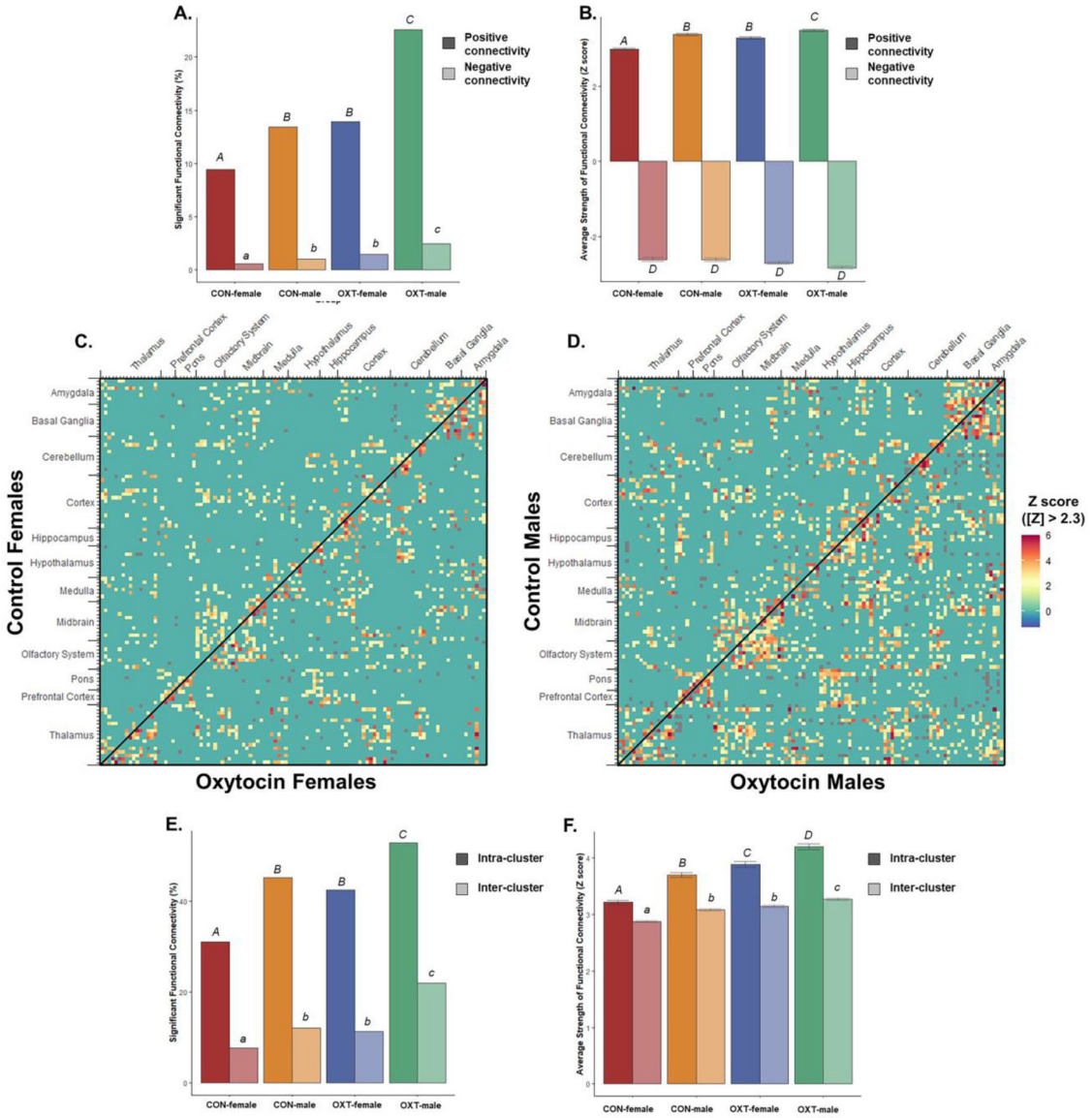

Figure 4.

Resting-state functional connectivity from 111 brain regions. (A) Both OXT treatment and male sex increased functional connectivity, meaning OXT-exposed males had the greatest proportion of region-region pairs significantly functionally connected for both positive (dark fill) and negative (light fill) correlations. Significant group differences are indicated with different letters over top the bars. (B) The average strength of correlation among region-region pairs whose activity was significantly correlated. Both OXT treatment and male sex increased the strength of connectivity for positive connections (dark fill). There were no significant differences among negative connections (light fill). (C) Both OXT treatment and male sex increased the strength of connectivity among both intra- and inter-cluster, though intra-cluster connectivity was more sensitive to these effects. Significant group differences are indicated with different letters over top the bars. In panels (D) and (E), connectivity from males and females respectively, 111x111 cell matrices show the strength

of connectivity for all possible pairs of brain regions. Reflected across the diagonal are opposing treatment conditions, with OXT on top and Control on bottom. Region-region pairs whose connectivity Z score was less than |2.3| were excluded.

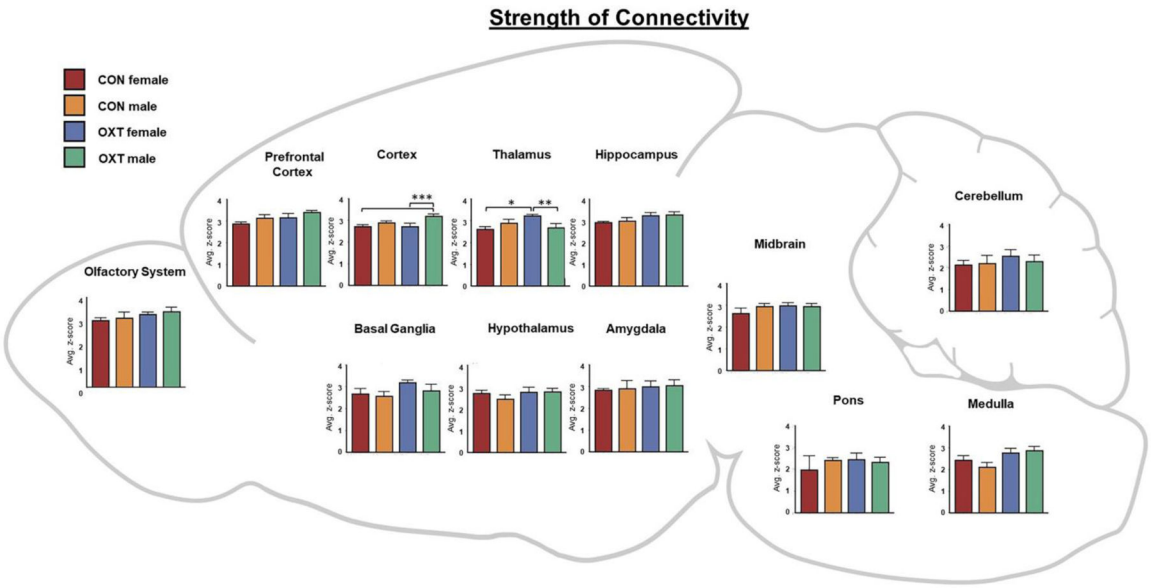

Figure 5.

A map of the strength of connectivity (i.e. correlations' z-scores) averaged over regional clusters by group. For example, the 'Hippocampus' cluster includes the: CA1, CA3, Dentate gyrus, Subiculum and Parasubiculum. * $p < 0.05$, ** $p < 0.01$, *** $p < 0.001$.

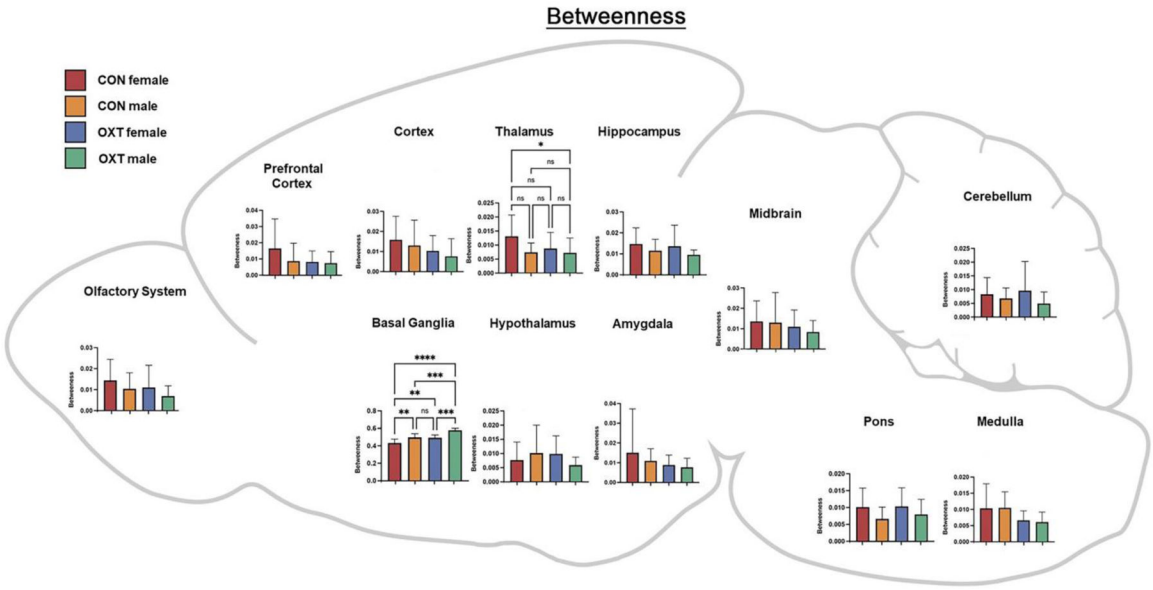

Figure 6.

A map of betweenness averaged over regional clusters by group. For example, the 'Hippocampus' cluster includes the: CA1, CA3, Dentate gyrus, Subiculum and Parasubiculum. * $p < 0.0332$, ** $p < 0.0021$, *** $p < 0.0002$, **** $p < 0.0001$.

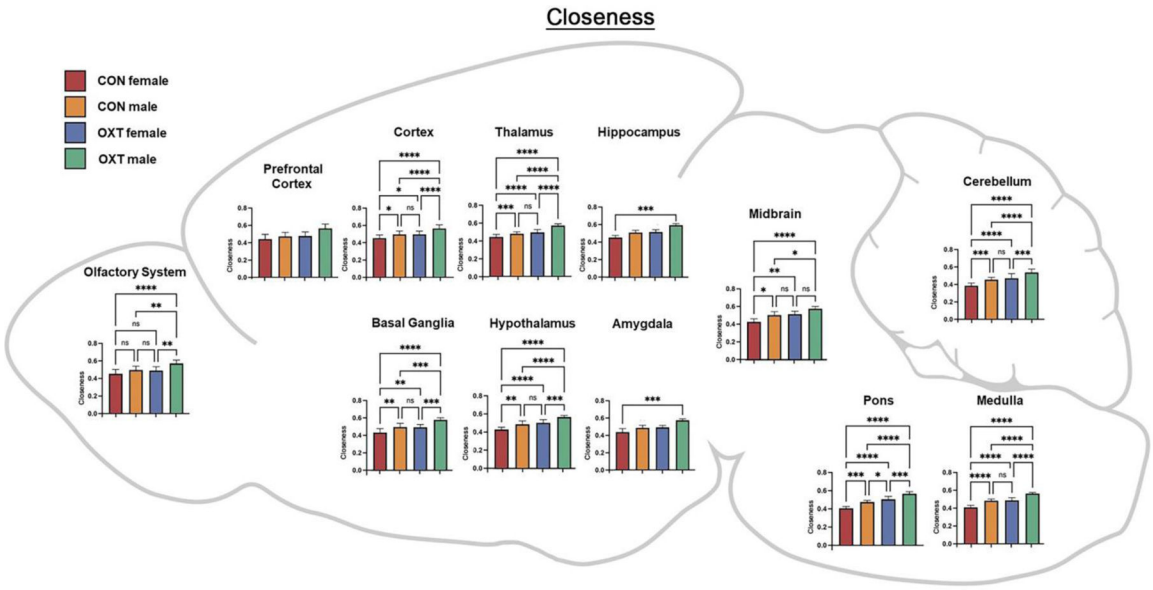

Figure 7.

A map of closeness averaged over regional clusters by group. Both OXT treatment and male sex increased closeness throughout the brain, with effects most apparent in OXT-exposed males. * $p < 0.0332$, ** $p < 0.0021$, *** $p < 0.0002$, **** $p < 0.0001$.

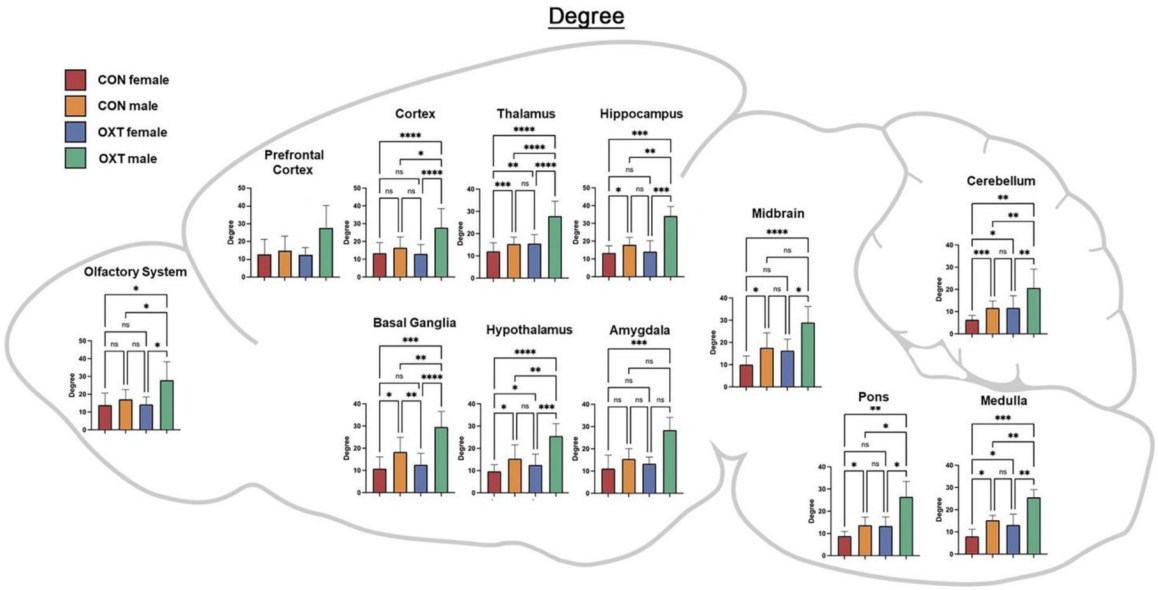

Figure 8.

A map of degree averaged over regional clusters by group. Both OXT treatment and male sex increased closeness throughout the brain, with effects most apparent in OXT-exposed males. * $p < 0.0332$, ** $p < 0.0021$, *** $p < 0.0002$, **** $p < 0.0001$.

Table 1.

A) a list of the single brain area, reticular nucleus of the thalamus, that significantly differs (p=0.021, critical value p<0.05) in volume between adult female and male voles that were treated with saline vehicle within 24 hrs of parturition. Shown are the average and standard deviation in volume in mm3 and effects size (omega square ωSq). With a false discovery rate (FDR) p=0.0017 this singular finding can be dismissed concluding there is no sex difference in brain volumes between female and male voles resulting following the OXT manipulation used here. In contrast, Table 1B lists the brain areas that are significantly different in volume between adult female and male voles exposed to OXT during birth (FDR p=0.043). The brain areas are ranked in order of significance and are truncated from a larger list of 116 areas taken from the vole MRI atlas (see Supplementary Table S1).

A	Female Vehicle vs Male Vehicle - Brain Volumes (mm3)							
		Female			Male			
	Brain Area	Ave	SD		Ave	SD	P-val	ω Sq
	reticular n.	2.6	0.4	>	2.3	0.3	0.021	*0.167325*

B	Female Oxytocin vs Male Oxytocin - Brain Volumes (mm3)							
		Female			Male			
	Brain Area	Ave	SD		Ave	SD	P-val	ω Sq
	frontal association ctx	12.4	3.1	>	9.7	2.8	0.003	*0.168232*
	ventral tegmental area	0.6	0.2	<	0.8	0.3	0.008	*0.134096*
	vestibular n.	1.5	0.6	<	2.2	0.8	0.009	*0.12879*
	agranular insular ctx	11.6	2.7	>	9.7	2.5	0.010	*0.127444*
	retrosplenial ctx	7.5	0.8	>	6.7	1.0	0.014	*0.112513*
	gigantocellular reticular n.	5.1	1.3	<	5.8	1.6	0.017	*0.104148*
	median raphe n.	0.5	0.2	<	0.8	0.4	0.019	*0.100934*
	secondary motor ctx	13.1	2.2	>	11.4	2.5	0.019	*0.100645*
	anterior hypothalamus	3.6	0.9	>	3.1	1.0	0.019	*0.099491*
	parasubiculum	1.4	0.4	<	1.8	0.5	0.021	*0.096134*
	paraflocculus cerebellum	5.4	1.7	<	6.1	1.6	0.022	*0.094944*
	cuneate n.	0.1	0.2	<	0.4	0.5	0.026	*0.087519*
	parietal ctx	2.5	0.7	>	2.1	0.6	0.029	*0.083929*
	7th cerebellar lobule	0.6	1.4	<	2.3	2.8	0.031	*0.08128*
	claustrum	1.9	0.5	>	1.5	0.6	0.031	*0.080768*
	medullary reticular n.	0.9	2.2	<	2.7	3.4	0.036	*0.07577*
	olivary n.	1.1	0.6	<	1.5	0.7	0.036	*0.075573*
	rostral piriform ctx	11.9	1.7	>	10.5	2.3	0.039	*0.072415*
	reticulotegmental n.	1.9	0.7	<	2.3	0.6	0.041	*0.07042*
	pontine reticular n. oral	2.0	0.8	<	2.7	1.2	0.042	*0.069447*
	anterior olfactory n.	14.1	2.1	>	12.2	2.8	0.045	*0.067423*
	anterior cingulate ctx	4.1	1.1	>	3.5	0.8	0.045	*0.067423*
	glomerular layer olfactory bulb	16.6	2.9	>	15.2	2.9	0.046	*0.066422*
	lateral preoptic area	1.4	0.3	>	1.2	0.4	0.052	*0.061681*
	caudal piriform ctx	9.0	1.4	>	8.3	1.2	0.052	*0.061604*

Table 2.

The list of brain regions that were significantly different in volume between OXT-exposed females and Control females. OXT-exposed females showed smaller brain volumes in 15/21 of the affected regions (FDR p=0.036). The regions affected spread across the olfactory system (anterior olfactory nuc., piriform cortex), hypothalamus (paraventricular, anterior), amygdala (basal, extended), thalamus (anterior, paraventricular) and basal ganglia (nuc. accumbens, caudate putamen).

Female Vehicle vs Female Oxytocin - Brain Volumes (mm3)							
	Female Veh			Female OT			
Brain Area	Ave	SD		Ave	SD	P-val	ω Sq
tegmental n.	1.3	0.3	>	0.9	0.3	0.000	*0.345836*
paraventricular hypothalamus	0.7	0.2	>	0.4	0.2	0.001	*0.284466*
anterior thalamus	2.2	0.7	>	1.5	0.5	0.005	*0.207551*
anterior hypothalamus	4.5	0.9	>	3.6	0.9	0.007	*0.187938*
accumbens shell	4.5	1.5	>	3.3	1.0	0.009	*0.174539*
caudate putamen (striatum)	25.7	4.1	>	22.2	3.4	0.010	*0.169285*
solitary tract n.	0.2	0.3	<	0.5	0.4	0.012	*0.157301*
5th cerebellar lobule	2.3	2.5	<	4.8	2.3	0.015	*0.144533*
basal amygdala	5.7	0.8	>	4.9	0.8	0.016	*0.141848*
anterior olfactory n.	16.4	2.9	>	14.1	2.1	0.019	*0.132333*
paraventricular thalamus	1.2	0.3	>	1.0	0.3	0.022	*0.125592*
rostral piriform ctx	14.2	2.9	>	11.9	1.7	0.025	*0.118632*
extended amydala	2.4	1.0	>	1.8	0.6	0.026	*0.116508*
orbital ctx	17.7	5.9	>	12.6	3.9	0.026	*0.116343*
trigeminal complex medulla	2.6	1.8	<	4.1	1.7	0.035	*0.101347*
primary motor ctx	13.3	2.6	>	11.4	1.9	0.035	*0.101255*
vestibular n.	2.0	0.8	>	1.5	0.6	0.037	*0.099219*
diagonal band of Broca	0.4	0.3	<	0.6	0.3	0.038	*0.097323*
red n.	0.5	0.2	<	0.7	0.2	0.047	*0.087375*
primary somatosensory ctx	26.0	3.0	>	24.1	3.3	0.047	*0.086965*
habenula n.	0.5	0.2	<	0.7	0.2	0.049	*0.085284*

Table 3.

The list of brain regions that were significantly different in volume between OXT-exposed males and Control males (FDR p=0.06). Males were most affected by OXT a birth showing 35/116 brain regions with significant differences from vehicle controls. As in the case of the females exposed to OXT at birth, the majority of the affected brain regions in OXT-exposed males were smaller than vehicle controls. The regions most sensitive were many of the same for females e.g. olfactory system, limbic cortex, basal ganglia, striatum, amygdala, and hypothalamus. The brain regions that were significantly larger in volume with OXT exposure were in the cerebellum (5th, 7th,8th, 9th lobules) and brainstem (gigantocellularis, trigeminal complex, cuneate nuc., medullary reticular nuc. pontine nuc.).

Male Vehicle vs Male Oxytocin - Brain Volumes (mm3)							
	Male Veh			Male OT			
Brain Area	Ave	SD		Ave	SD	P-val	ω Sq
frontal association ctx	13.4	1.9	>	9.7	2.8	0.000	*0.32943*
agranular insular ctx	13.6	3.8	>	9.7	2.5	0.002	*0.22789*
claustrum	2.4	1.0	>	1.5	0.6	0.003	*0.21273*
rostral piriform ctx	13.2	2.4	>	10.5	2.3	0.003	*0.20768*
anterior olfactory n.	14.9	1.8	>	12.2	2.8	0.004	*0.1931*
5th cerebellar lobule	2.7	2.8	<	5.4	2.1	0.005	*0.19098*
endopiriform n.	4.6	1.4	>	3.5	0.8	0.006	*0.17671*
primary somatosensory ctx	25.4	3.3	>	22.1	3.2	0.006	*0.17439*
7th cerebellar lobule	0.3	0.9	<	2.3	2.8	0.007	*0.17291*
accumbens core	2.3	0.7	>	1.7	0.5	0.007	*0.16991*
granular cell layer olfactory bulb	11.4	3.5	>	9.0	1.2	0.008	*0.16111*
orbital ctx	15.7	6.0	>	11.0	2.8	0.011	*0.14783*
globus pallidus	3.5	0.6	>	2.8	0.6	0.012	*0.14374*
caudate putamen (striatum)	25.0	4.6	>	21.3	3.7	0.012	*0.14359*
glomerular layer olfactory bulb	18.9	4.9	>	15.2	2.9	0.013	*0.13943*
cortical amygdala	3.5	0.5	>	3.0	0.6	0.016	*0.12943*
retrosplenial ctx	7.6	1.1	>	6.7	1.0	0.016	*0.12923*
9th cerebellar lobule	0.1	0.4	<	1.4	1.9	0.018	*0.12523*
cuneate n.	0.0	0.1	<	0.4	0.5	0.018	*0.12523*
trigeminal complex	3.1	2.6	<	4.5	1.5	0.019	*0.12132*
secondary somatosensory ctx	6.2	1.0	>	5.2	1.0	0.019	*0.1213*
visual 2 ctx	9.0	1.0	>	8.1	1.4	0.020	*0.11941*
zona incerta	1.6	0.2	<	1.8	0.3	0.022	*0.11573*
dentate gyrus	8.1	0.4	>	7.5	1.1	0.022	*0.11556*
basal amygdala	5.2	0.7	>	4.5	0.9	0.025	*0.10986*
anterior cingulate ctx	4.2	0.9	>	3.5	0.8	0.026	*0.10789*
caudal piriform ctx	9.3	1.1	>	8.3	1.2	0.027	*0.10603*
anterior thalamus	2.0	0.8	>	1.3	0.4	0.029	*0.10239*
gigantocellular reticular n.	4.2	2.4	<	5.8	1.6	0.031	*0.09872*
central amygdaloid n.	2.3	0.3	>	2.0	0.5	0.032	*0.09704*

Male Vehicle vs Male Oxytocin - Brain Volumes (mm3)							
	Male Veh			Male OT			
Brain Area	**Ave**	**SD**		**Ave**	**SD**	**P-val**	**ω Sq**
anterior hypothalamic area	3.9	1.3	>	3.1	1.0	0.034	*0.09515*
medullary reticular n.	0.7	2.5	<	2.7	3.4	0.038	*0.08917*
8th cerebellar lobule	0.3	1.1	<	1.6	1.9	0.039	*0.08829*
pontine n.	0.5	0.2	<	0.6	0.2	0.047	*0.07992*
infralimbic ctx	1.0	0.3	>	0.7	0.5	0.047	*0.0797*

Table 4.

The list of brain regions that were significantly different in fractional anisotropy between OXT-exposed females and Control females.

Fractional Anisotropy: Control Females vs Oxytocin Females						
Brain Area	**Female Control**		**Female Oxytocin**			
	Mean	**SD**	**Mean**	**SD**	**P val**	**Effect**
3rd cerebellar lobule	0.4825	0.0609	0.5259	0.0582	0.0235	*0.117822*
5th cerebellar lobule	0.489	0.0585	0.5273	0.0573	0.0388	*0.103671*
anterior cingulate ctx	0.478	0.0515	0.5141	0.0609	0.044	*0.100389*
inferior colliculus	0.4405	0.0436	0.4718	0.0561	0.0492	*0.094993*
auditory ctx	0.4565	0.0437	0.4886	0.0457	0.025	*0.094146*

Table 5.

The list of brain regions that were significantly different in fractional anisotropy (FA) between OXT-exposed males and Control males. While widespread, differences were generally small in effect, with OXT-exposed males generally showing greater FA scores.

Fractional Anisotropy: Control Males vs Oxytocin Males							
Brain Area	**Males Control**			**Males Oxytocin**			
	Mean	**SD**		**Mean**	**SD**	**P val**	**Effect**
medial preoptic area	0.47	0.06	<	0.52	0.06	0.004	*0.124903*
pontine nuclei	0.50	0.07	<	0.53	0.04	0.001	*0.091476*
medial geniculate	0.55	0.06	<	0.59	0.05	0.024	*0.07966*
median raphe nucleus	0.52	0.05	<	0.56	0.06	0.015	*0.079723*
lateral geniculate	0.52	0.06	<	0.56	0.05	0.009	*0.082289*
parabrachial nucleus	0.51	0.03	<	0.53	0.05	0.012	*0.058617*
lateral dorsal thalamic nucleus	0.50	0.06	<	0.53	0.05	0.005	*0.079003*
reticular formation	0.52	0.05	<	0.54	0.05	0.002	*0.067602*
lemniscal nucleus	0.55	0.03	<	0.57	0.04	0.002	*0.047455*
anterior olfactory nucleus	0.48	0.07	<	0.51	0.03	0.023	*0.071355*
3rd cerebellar lobule	0.51	0.04	<	0.53	0.04	0.001	*0.047575*
ventral pallidum	0.46	0.04	<	0.49	0.06	0.026	*0.071662*
ventral medial nucleus	0.56	0.05	>	0.53	0.05	0.015	*0.062455*
reuniens nucleus	0.48	0.05	<	0.51	0.05	0.043	*0.06446*
trigeminal complex pons	0.51	0.06	<	0.53	0.06	0.007	*0.066325*
agranular insular ctx	0.55	0.06	<	0.57	0.04	0.014	*0.052015*
cortical amygdaloid nucleus	0.52	0.06	<	0.54	0.05	0.037	*0.058075*
auditory ctx	0.49	0.04	<	0.51	0.04	0.049	*0.046308*
medial amygdaloid nucleus	0.47	0.06	>	0.44	0.08	0.032	*0.085575*
periaqueductal gray	0.51	0.06	<	0.53	0.06	0.023	*0.056552*
ventral thalamic nuclei	0.50	0.05	<	0.53	0.07	0.027	*0.058593*
2nd cerebellar lobule	0.47	0.05	<	0.50	0.08	0.005	*0.063622*
posterior thalamic nucleus	0.52	0.06	<	0.54	0.04	0.006	*0.043435*
paraventricular nucleus, hypothalamus	0.48	0.06	<	0.50	0.07	0.009	*0.055935*
superior colliculus	0.45	0.04	<	0.46	0.06	0.012	*0.050091*
reticulotegmental nucleus	0.53	0.05	<	0.54	0.04	0.009	*0.031722*
frontal association ctx	0.53	0.05	<	0.55	0.05	0.049	*0.036404*
prelimbic ctx	0.53	0.05	<	0.54	0.04	0.047	*0.028273*
olivary nucleus	0.48	0.06	<	0.50	0.05	0.036	*0.040708*
central medial thalamic nucleus	0.52	0.05	<	0.54	0.06	0.017	*0.038405*
Ventricle	0.52	0.06	<	0.54	0.06	0.029	*0.042143*
reticular nucleus	0.48	0.07	<	0.50	0.05	0.033	*0.044729*
lateral preoptic area	0.52	0.05	<	0.53	0.04	0.001	*0.030365*
tegmental nucleus	0.50	0.05	<	0.52	0.07	0.011	*0.03654*
CA3	0.49	0.04	<	0.50	0.04	0.024	*0.024621*

Fractional Anisotropy: Control Males vs Oxytocin Males							
Brain Area	**Males Control**			**Males Oxytocin**			
	Mean	**SD**		**Mean**	**SD**	**P val**	**Effect**
lateral amygdaloid nucleus	0.50	0.04	<	0.51	0.07	0.028	*0.036617*
nucleus lateral olfactory tract	0.46	0.04	<	0.47	0.06	0.047	*0.029911*
medial dorsal thalamic nucleus	0.48	0.04	<	0.48	0.06	0.040	*0.024701*
subiculum	0.53	0.05	<	0.54	0.04	0.014	*0.019047*
8th cerebellar lobule	0.49	0.05	<	0.50	0.06	0.029	*0.023925*
CA1	0.48	0.03	<	0.49	0.06	0.042	*0.019205*
lateral septal nucleus	0.52	0.08	<	0.53	0.07	0.011	*0.026644*
accumbens shell	0.51	0.06	<	0.52	0.06	0.012	*0.021319*
entorhinal ctx	0.45	0.05	<	0.46	0.07	0.017	*0.024468*
paraflocculus cerebellum	0.50	0.03	>	0.49	0.07	0.047	*0.019452*
extended amydala	0.53	0.05	<	0.54	0.04	0.003	*0.015815*
inferior colliculus	0.47	0.04	<	0.47	0.07	0.008	*0.020534*
endopiriform nucleus	0.44	0.05	<	0.44	0.07	0.041	*0.02301*
visual 2 ctx	0.53	0.08	<	0.54	0.06	0.045	*0.018208*
substantia nigra	0.52	0.06	<	0.52	0.05	0.010	*0.012212*
central amygdaloid nucleus	0.45	0.04	<	0.45	0.06	0.037	*0.012965*
olfactory tubercles	0.49	0.08	<	0.50	0.07	0.034	*0.011715*
retrosplenial ctx	0.50	0.03	>	0.50	0.06	0.024	*0.007609*
7th cerebellar lobule	0.49	0.06	<	0.50	0.06	0.046	*0.008682*
lateral hypothalamus	0.45	0.05	<	0.45	0.07	0.033	*0.007054*
diagonal band of Broca	0.50	0.04	<	0.50	0.05	0.007	*0.003926*
mammillary nucleus	0.46	0.05	<	0.46	0.07	0.028	*0.003179*

Table 6.

The list of brain regions that were significantly different in fractional anisotropy (FA) between Control females and Control males. While widespread, differences outside of the thalamus were generally small in effect, with females generally showing greater FA scores.

Fractional Anisotropy: Control Females and Males							
Brain Area	**Females (n=17)**			**Males (n=19)**			
	Mean	**SD**		**Mean**	**SD**	**P val**	**Effect**
parafascicular thalamic nucleus	0.48	0.06	>	0.39	0.07	0.000	*0.324472*
habenula nucleus	0.49	0.07	>	0.41	0.08	0.001	*0.291157*
lateral geniculate	0.56	0.05	>	0.47	0.07	0.000	*0.261072*
bed nucleus stria terminalis	0.48	0.04	>	0.41	0.05	0.000	*0.260134*
diagonal band of Broca	0.48	0.04	>	0.40	0.08	0.002	*0.240761*
claustrum	0.47	0.06	>	0.40	0.06	0.003	*0.230304*
lateral dorsal thalamic nucleus	0.58	0.05	>	0.51	0.10	0.005	*0.210171*
glomerular layer olfactory bulb	0.48	0.03	>	0.42	0.07	0.002	*0.199748*
lateral amygdaloid nucleus	0.50	0.08	>	0.43	0.08	0.020	*0.198068*
granular cell layer olfactory bulb	0.46	0.04	>	0.40	0.07	0.004	*0.197001*
central medial thalamic nucleus	0.51	0.06	>	0.44	0.08	0.010	*0.191312*
pretectal nucleus	0.48	0.04	>	0.42	0.06	0.001	*0.190049*
ventral tegmental area	0.57	0.06	>	0.50	0.07	0.003	*0.186418*
anterior olfactory nucleus	0.48	0.03	>	0.42	0.06	0.001	*0.182102*
medial geniculate	0.52	0.04	>	0.46	0.08	0.005	*0.180481*
olfactory tubercles	0.52	0.03	>	0.46	0.07	0.002	*0.178895*
6th cerebellar lobule	0.48	0.05	>	0.42	0.06	0.003	*0.178003*
medial preoptic area	0.51	0.03	>	0.45	0.08	0.006	*0.177545*
caudate putamen (striatum)	0.47	0.05	>	0.41	0.06	0.008	*0.176083*
posterior hypothalamic area	0.54	0.07	>	0.48	0.05	0.005	*0.175232*
orbital ctx	0.45	0.04	>	0.40	0.06	0.006	*0.17508*
tegmental nucleus	0.55	0.08	>	0.49	0.07	0.017	*0.171393*
reuniens nucleus	0.54	0.06	>	0.48	0.07	0.008	*0.170836*
dorsal raphe	0.52	0.07	>	0.46	0.08	0.024	*0.170389*
tenia tecta ctx	0.51	0.03	>	0.45	0.07	0.005	*0.170225*
red nucleus	0.53	0.06	>	0.47	0.07	0.010	*0.168993*
medial septum	0.48	0.07	>	0.43	0.07	0.035	*0.168928*
CA1	0.51	0.04	>	0.45	0.06	0.003	*0.168383*
posterior thalamic nucleus	0.52	0.03	>	0.46	0.07	0.004	*0.166535*
anterior thalamic nuclei	0.45	0.05	>	0.40	0.06	0.013	*0.16469*
substantia nigra	0.60	0.05	>	0.53	0.06	0.002	*0.162592*
secondary somaotsensory ctx	0.45	0.05	>	0.40	0.07	0.027	*0.158391*
lateral posterior thalamic nucleus	0.51	0.06	>	0.45	0.07	0.025	*0.155251*
CA3	0.53	0.04	>	0.47	0.07	0.007	*0.152723*
reticular formation	0.52	0.05	>	0.47	0.06	0.012	*0.15052*

Fractional Anisotropy: Control Females and Males							
Brain Area	**Females (n=17)**			**Males (n=19)**			
	Mean	**SD**		**Mean**	**SD**	**P val**	**Effect**
dorsal medial nucleus	0.53	0.06	>	0.48	0.07	0.020	*0.145566*
accumbens core	0.53	0.04	>	0.48	0.06	0.003	*0.144539*
subiculum	0.49	0.04	>	0.45	0.06	0.011	*0.139425*
dentate gyrus	0.49	0.04	>	0.45	0.07	0.015	*0.137887*
ventral pallidum	0.53	0.04	>	0.48	0.06	0.008	*0.137735*
superior colliculus	0.44	0.04	>	0.40	0.06	0.019	*0.13266*
lateral preoptic area	0.56	0.04	>	0.51	0.08	0.023	*0.132598*
extended amydala	0.52	0.06	>	0.47	0.06	0.020	*0.131951*
parasubiculum	0.44	0.04	>	0.40	0.07	0.037	*0.131038*
median raphe nucleus	0.59	0.05	>	0.54	0.08	0.026	*0.130939*
interpeduncular nucleus	0.54	0.05	>	0.50	0.05	0.011	*0.130127*
7th cerebellar lobule	0.52	0.05	>	0.47	0.06	0.022	*0.130134*
accumbens shell	0.52	0.05	>	0.48	0.06	0.018	*0.12372*
zona incerta	0.64	0.05	>	0.58	0.07	0.018	*0.119864*
central amygdaloid nucleus	0.53	0.06	>	0.49	0.07	0.049	*0.119507*
8th cerebellar lobule	0.53	0.05	>	0.49	0.05	0.018	*0.119381*
endopiriform nucleus	0.49	0.06	>	0.45	0.05	0.046	*0.11912*
parabrachial nucleus	0.54	0.05	>	0.50	0.06	0.024	*0.117299*
paraventricular nuclus	0.55	0.06	>	0.50	0.07	0.040	*0.116178*
basal amygdaloid nucleus	0.56	0.05	>	0.51	0.07	0.046	*0.115372*
ventral thalamic nuclei	0.55	0.04	>	0.51	0.06	0.020	*0.115201*
9th cerebellar lobule	0.53	0.06	>	0.49	0.05	0.040	*0.108169*
pontine reticular nucleus oral	0.55	0.05	>	0.51	0.06	0.027	*0.107503*
cortical amygdaloid nucleus	0.53	0.04	>	0.50	0.06	0.040	*0.101249*
trigeminal complex medulla	0.53	0.02	>	0.49	0.05	0.007	*0.099082*
reticulotegmental nucleus	0.55	0.05	>	0.51	0.05	0.041	*0.095013*
crus ansiform lobule	0.50	0.04	>	0.47	0.05	0.040	*0.089621*

Table 7.

The list of brain regions that were significantly different in apparent diffusion coefficient (ADC) between Control females and Control males. While widespread, differences were generally small in effect, with males generally showing greater ADC scores.

Apparent Diffusion Coefficient: Control Females and Males							
Brain Area	**Females**			**Males**			
	Mean	**SD**		**Mean**	**SD**	**P val**	**Effect**
cuneate nucleus	1.27	0.11	<	1.48	0.29	0.008	*0.191902*
9th cerebellar lobule	1.31	0.15	<	1.52	0.28	0.009	*0.186984*
tegmental nucleus	1.29	0.15	<	1.49	0.16	0.000	*0.184923*
7th cerebellar lobule	1.13	0.09	<	1.29	0.28	0.025	*0.172738*
parafascicular thalamic nucleus	1.24	0.11	<	1.41	0.18	0.001	*0.171383*
central medial thalamic nucleus	1.22	0.09	<	1.40	0.18	0.001	*0.170847*
dentate gyrus	1.40	0.15	<	1.60	0.22	0.003	*0.170166*
red nucleus	1.26	0.14	<	1.44	0.19	0.003	*0.167449*
perirhinal ctx	1.34	0.15	<	1.52	0.24	0.009	*0.163461*
habenula nucleus	1.34	0.11	<	1.52	0.24	0.009	*0.156466*
central amygdaloid nucleus	1.32	0.11	<	1.49	0.18	0.002	*0.155197*
ventral tegmental area	1.45	0.23	<	1.64	0.30	0.045	*0.153921*
reticular nucleus	1.29	0.09	<	1.46	0.18	0.002	*0.15359*
caudate putamen (striatum)	1.23	0.09	<	1.39	0.18	0.002	*0.153054*
accumbens core	1.25	0.10	<	1.40	0.15	0.001	*0.149244*
posterior thalamic nucleus	1.24	0.11	<	1.39	0.17	0.004	*0.146364*
globus pallidus	1.22	0.10	<	1.37	0.17	0.004	*0.144324*
zona incerta	1.32	0.16	<	1.47	0.21	0.018	*0.143221*
lateral amygdaloid nucleus	1.40	0.14	<	1.56	0.20	0.008	*0.141691*
temporal ctx	1.30	0.13	<	1.45	0.21	0.016	*0.141549*
median raphe nucleus	1.33	0.16	<	1.48	0.21	0.019	*0.139344*
parabrachial nucleus	1.31	0.14	<	1.46	0.17	0.008	*0.137927*
medial geniculate	1.26	0.12	<	1.40	0.17	0.007	*0.136556*
basal amygdaloid nucleus	1.31	0.17	<	1.45	0.18	0.021	*0.13487*
pontine reticular nucleus oral	1.34	0.21	<	1.48	0.22	0.047	*0.13411*
pretectal nucleus	1.28	0.10	<	1.42	0.18	0.007	*0.132915*
reticular formation	1.33	0.14	<	1.47	0.19	0.015	*0.132011*
claustrum	1.23	0.11	<	1.36	0.17	0.009	*0.131793*
White Matter	1.37	0.11	<	1.51	0.20	0.011	*0.131328*
reuniens nucleus	1.28	0.13	<	1.42	0.18	0.015	*0.130902*
ventral thalamic nuclei	1.28	0.11	<	1.41	0.18	0.010	*0.130631*
subiculum	1.40	0.16	<	1.55	0.20	0.021	*0.128979*
dorsal raphe	1.35	0.14	<	1.49	0.20	0.020	*0.127819*
lateral septal nucleus	1.45	0.12	<	1.60	0.18	0.008	*0.123361*
auditory ctx	1.29	0.12	<	1.42	0.19	0.023	*0.120441*

Apparent Diffusion Coefficient: Control Females and Males							
Brain Area	**Females**			**Males**			
	Mean	**SD**		**Mean**	**SD**	**P val**	**Effect**
periaqueductal gray	1.41	0.11	<	1.55	0.22	0.027	*0.119783*
lateral posterior thalamic nucleus	1.30	0.10	<	1.43	0.17	0.012	*0.119406*
CA3	1.39	0.13	<	1.53	0.21	0.028	*0.118736*
posterior hypothalamic area	1.32	0.17	<	1.44	0.18	0.039	*0.118504*
infralimbic ctx	1.48	0.16	<	1.62	0.18	0.018	*0.117904*
CA1	1.40	0.12	<	1.53	0.19	0.017	*0.117489*
bed nucleus stria terminalis	1.30	0.13	<	1.43	0.17	0.019	*0.115845*
orbital ctx	1.36	0.14	<	1.48	0.21	0.046	*0.113322*
solitary tract nucleus	1.30	0.13	<	1.42	0.20	0.044	*0.113143*
paraventricular nuclus	1.37	0.15	<	1.49	0.16	0.022	*0.112125*
medial septum	1.34	0.14	<	1.46	0.14	0.022	*0.107011*
lateral geniculate	1.31	0.11	<	1.42	0.18	0.034	*0.106521*
extended amydala	1.33	0.15	<	1.44	0.17	0.043	*0.106481*

Table 8.

The list of brain regions that were significantly different in apparent diffusion coefficient (ADC) between OXT-exposed males and Control males. While widespread, differences were generally small in effect, with Control males generally showing greater ADC scores. Note: there were no regions where OXT-exposed females and Control females differed in terms of ADC.

Apparent Diffusion Coefficient: Control Males vs Oxytocin Males							
Brain Area	**Males Control**			**Males Oxytocin**			
	Mean	**SD**		**Mean**	**SD**	**P val**	**Effect**
periaqueductal gray	1.55	0.22	>	1.31	0.14	0.000	*0.252665*
tegmental nucleus	1.49	0.16	>	1.26	0.13	0.000	*0.243266*
vestibular nucleus	1.48	0.16	>	1.26	0.15	0.000	*0.228493*
dorsal raphe	1.49	0.20	>	1.28	0.14	0.000	*0.224489*
parafascicular thalamic nucleus	1.41	0.18	>	1.22	0.12	0.000	*0.221093*
reuniens nucleus	1.42	0.18	>	1.22	0.14	0.000	*0.221224*
paraventricular nuclus	1.49	0.16	>	1.29	0.13	0.000	*0.210742*
posterior thalamic nucleus	1.39	0.17	>	1.21	0.13	0.000	*0.20552*
superior colliculus	1.45	0.19	>	1.26	0.13	0.000	*0.203265*
ventral thalamic nuclei	1.41	0.18	>	1.23	0.14	0.000	*0.198616*
CA3	1.53	0.21	>	1.33	0.15	0.000	*0.201625*
central amygdaloid nucleus	1.49	0.18	>	1.31	0.14	0.000	*0.19427*
central medial thalamic nucleus	1.40	0.18	>	1.22	0.12	0.000	*0.198094*
lateral amygdaloid nucleus	1.56	0.20	>	1.39	0.13	0.000	*0.174127*
medial dorsal thalamic nucleus	1.40	0.19	>	1.22	0.14	0.000	*0.200707*
pretectal nucleus	1.42	0.18	>	1.25	0.12	0.000	*0.182947*
secondary somaotsensory ctx	1.42	0.17	>	1.27	0.13	0.000	*0.16995*
medial geniculate	1.40	0.17	>	1.24	0.14	0.000	*0.181864*
bed nucleus stria terminalis	1.43	0.17	>	1.26	0.13	0.000	*0.184272*
accumbens core	1.40	0.15	>	1.24	0.12	0.000	*0.178726*
CA1	1.53	0.19	>	1.36	0.15	0.000	*0.177719*
lateral dorsal thalamic nucleus	1.48	0.18	>	1.32	0.13	0.000	*0.166541*
parabrachial nucleus	1.46	0.17	>	1.30	0.16	0.000	*0.163127*
lateral posterior thalamic nucleus	1.43	0.17	>	1.26	0.14	0.000	*0.178745*
red nucleus	1.44	0.19	>	1.27	0.14	0.000	*0.187887*
primary somatosensory ctx	1.55	0.21	>	1.39	0.17	0.001	*0.150456*
reticular nucleus	1.46	0.18	>	1.29	0.13	0.001	*0.178808*
inferior colliculus	1.50	0.21	>	1.30	0.14	0.001	*0.204884*
habenula nucleus	1.52	0.24	>	1.35	0.19	0.001	*0.166456*
medial septum	1.46	0.14	>	1.29	0.13	0.001	*0.173046*
paraventricular nucleus	1.40	0.19	>	1.23	0.17	0.001	*0.189772*
White Matter	1.51	0.20	>	1.35	0.15	0.001	*0.160272*
lateral geniculate	1.42	0.18	>	1.25	0.13	0.001	*0.17768*
2nd cerebellar lobule	1.47	0.20	>	1.30	0.21	0.001	*0.174388*

Apparent Diffusion Coefficient: Control Males vs Oxytocin Males							
Brain Area	**Males Control**			**Males Oxytocin**			
	Mean	**SD**		**Mean**	**SD**	**P val**	**Effect**
caudate putamen (striatum)	1.39	0.18	>	1.23	0.12	0.001	*0.169379*
claustrum	1.36	0.17	>	1.21	0.11	0.001	*0.167135*
anterior thalamic nuclei	1.40	0.18	>	1.24	0.15	0.001	*0.174358*
median raphe nucleus	1.48	0.21	>	1.33	0.17	0.001	*0.148878*
reticular formation	1.47	0.19	>	1.31	0.19	0.001	*0.162688*
accumbens shell	1.43	0.16	>	1.26	0.14	0.002	*0.181389*
auditory ctx	1.42	0.19	>	1.27	0.16	0.002	*0.1609*
globus pallidus	1.37	0.17	>	1.21	0.14	0.002	*0.171928*
orbital ctx	1.48	0.21	>	1.31	0.14	0.003	*0.173424*
infralimbic ctx	1.62	0.18	>	1.44	0.16	0.003	*0.162521*
7th cerebellar lobule	1.29	0.28	>	1.08	0.18	0.003	*0.263639*
visual 1 ctx	1.50	0.25	>	1.34	0.19	0.003	*0.158911*
anterior olfactory nucleus	1.57	0.30	>	1.35	0.22	0.003	*0.213927*
10th cerebellar lobule	1.62	0.25	>	1.43	0.17	0.003	*0.180961*
dentate gyrus	1.60	0.22	>	1.41	0.19	0.003	*0.180572*
agranular insular ctx	1.45	0.17	>	1.30	0.23	0.004	*0.157405*
5th cerebellar lobule	1.25	0.24	>	1.07	0.19	0.004	*0.229309*
extended amydala	1.44	0.17	>	1.29	0.17	0.004	*0.152473*
3rd cerebellar lobule	1.30	0.22	>	1.13	0.21	0.004	*0.203067*
endopiriform nucleus	1.40	0.18	>	1.26	0.18	0.005	*0.153927*
6th cerebellar lobule	1.24	0.23	>	1.03	0.18	0.005	*0.262008*
parasubiculum	1.57	0.28	>	1.42	0.21	0.005	*0.149793*
subiculum	1.55	0.20	>	1.40	0.24	0.007	*0.137179*
frontal association ctx	1.58	0.24	>	1.43	0.19	0.008	*0.150833*
zona incerta	1.47	0.21	>	1.31	0.22	0.011	*0.17364*
temporal ctx	1.45	0.21	>	1.30	0.22	0.012	*0.158125*
lateral septal nucleus	1.60	0.18	>	1.48	0.12	0.012	*0.109379*
primary motor ctx	1.60	0.27	>	1.49	0.19	0.014	*0.094467*
visual 2 ctx	1.66	0.31	>	1.52	0.20	0.015	*0.122483*
ventral pallidum	1.47	0.18	>	1.32	0.18	0.015	*0.151041*
pontine reticular nucleus oral	1.48	0.22	>	1.36	0.27	0.016	*0.122237*
solitary tract nucleus	1.42	0.20	>	1.28	0.21	0.016	*0.148623*
retrosplenial ctx	1.77	0.33	>	1.64	0.22	0.016	*0.106864*
basal amygdaloid nucleus	1.45	0.18	>	1.30	0.23	0.022	*0.162508*
anterior hypothalamic area	1.55	0.23	>	1.39	0.27	0.023	*0.159099*
9th cerebellar lobule	1.52	0.28	>	1.33	0.19	0.024	*0.188268*
posterior hypothalamic area	1.44	0.18	>	1.28	0.16	0.024	*0.170827*
medial preoptic area	1.57	0.25	>	1.41	0.23	0.024	*0.157191*
diagonal band of Broca	1.53	0.22	>	1.40	0.21	0.025	*0.134138*
pontine reticular nucleus caudal	1.49	0.22	>	1.38	0.34	0.025	*0.1033*

Apparent Diffusion Coefficient: Control Males vs Oxytocin Males							
Brain Area	**Males Control**			**Males Oxytocin**			
	Mean	**SD**		**Mean**	**SD**	**P val**	**Effect**
perirhinal ctx	1.52	0.24	>	1.36	0.31	0.028	*0.166175*
anterior cingulate ctx	1.75	0.24	>	1.58	0.20	0.028	*0.14404*
crus ansiform lobule	1.36	0.24	>	1.23	0.23	0.029	*0.151202*
8th cerebellar lobule	1.38	0.29	>	1.23	0.24	0.034	*0.162496*
gigantocellular reticular nucleus	1.53	0.26	>	1.43	0.38	0.036	*0.10108*
granular cell layer olfactory bulb	1.56	0.30	>	1.40	0.16	0.040	*0.160613*
cuneate nucleus	1.48	0.29	>	1.34	0.25	0.042	*0.140914*
dorsal medial nucleus	1.64	0.25	>	1.51	0.20	0.046	*0.11454*
medial amygdaloid nucleus	1.68	0.25	>	1.52	0.34	0.049	*0.135506*